JOURNAL OF CATALYSIS 155, 219–237 (1995)

Reactions of Acetaldehyde on CeO_2 and CeO_2-Supported Catalysts

H. Idriss,*,[1] C. Diagne,†,[2] J. P. Hindermann,† A. Kiennemann,† and M. A. Barteau*

*Department of Chemical Engineering, Center for Catalytic Science and Technology, University of Delaware, Newark, Delaware 19716; and †LERCSI-EHICS, Laboratoire Etude de la Réaction Catalytique des Surfaces et Interfaces, 1 rue Blaise Pascal, 67008 Strasbourg CEDEX, France

Received September 12, 1994; revised March 16, 1995

The reactions of acetaldehyde were investigated on the surfaces of CeO_2, 3 wt% Pd/CeO_2, 3 wt% Co/CeO_2, and 3 wt% Pd–3 wt% Co/CeO_2 by temperature programmed desorption (TPD) and infrared spectroscopy (FT-IR). The surface and bulk compositions of these catalysts were studied by X-ray photoelectron spectroscopy (XPS), X-ray diffraction (XRD), and CO chemisorption. XRD patterns indicated that the fluorite structure of CeO_2 was maintained in all catalysts (calcined and H_2-reduced) and that there were no apprediable differences in particle dimension between CeO_2 alone (96 Å) and metal/CeO_2 catalysts (84–98 Å). Reduced catalysts were investigated by XPS: Ce (3*d*) spectra indicated the precence of Ce^{3+} cations, evidenced by V′ and U′ peaks at 885.0 and 903.7 eV, together with Ce^{4+} species. Co 2*p* spectra indicated the presence of Co^{2+} cations, evidenced by the Co $2p_{3/2}$ line at 781.0 eV (and its satellite at about 788 eV) and Co $2p_{1/2}$ at 797.0 eV (and its satellite at about 804 eV). Pd metal was detected on Pd/CeO_2 and Pd–Co/CeO_2. Several reactions of acetaldehyde were observed; they can be classified as oxidation, reduction, or carbon–carbon bond formation reactions. Oxidation to acetates and reduction to ethanol were observed on all catalysts; acetate species were identified by their IR bands at 1560–1540, 1451, 1400, 1343, and 1020 cm^{-1} at room temperature, and ethanol was observed to desorb at ca. 400 K during acetaldehyde TPD. Several other adsorbed species were observed (on hydrogen reduced catalysts) by IR: acetyl, fingerprinted by a 1684 cm^{-1} band on metal/CeO_2, η^2 (C, O) acetaldehyde (bands at 1220–1268, 1175–1156, 950–940 cm^{-1}) on Pd/CeO_2 and Pd–Co/CeO_2, and CO adsorbed by its carbon to metal (Pd, Co) and by its oxygen to reduced Ce, giving rise to bands at 1730, 1739, and 1750 cm^{-1}. Four C–C bond formation reactions were observed: (1) β-aldolization to crotonaldehyde and crotyl alcohol (most prominent on CeO_2 alone), (2) acetate ketonization to acetone and CO_2 on CeO_2 and Co/CeO_2, (3) acetyl reaction with methyl species to give acetone on Pd/CeO_2, Co/CeO_2, and Pd–Co/CeO_2 (this acetone desorption was coincident with propane desorption on Pd/CeO_2 and Co/CeO_2), (4) reductive coupling of two molecules of acetaldehyde to butene and butadiene (on CeO_2 and Co/CeO_2). Pd–Co/CeO_2 adsorbed four times more CO than did Pd/CeO_2 or Co/CeO_2 and was the most active for acetaldehyde conversion.

INTRODUCTION

The reactions of oxygenated hydrocarbons require systematic study for both fundmental and applied reasons. Because of environmental considerations, atmospheric chemists are studying their noncatalytic reactions in the gas phase, in order to assess the consequences of the use of oxygenates as fuels and fuel additives (1–3). In addition, the search for better catalytic converters has motivated studies of total combustion of these oxygenates (4–8). Among several families of oxygenates, aldehydes are particularly undesirable in exhaust because of their potential carcinogenic effects (9). The most abundant aldehydes in atmospheric studies are formaldehyde and acetaldehyde (10).

Since acetaldehyde can be produced from partial oxidation of ethanol or its corresponding ethers (such as diethyl ether and ethyl tertiarybutyl ether) and because these oxygenates are used as fuels, it is worthwhile to study the mechanisms of its formation and reactions on solid surfaces as well as in the gas phase. The complexity of the gas–solid catalytic and noncatalytic chemistry of acetaldehyde on both metals and metal oxides is the driving force for the present study.

Aldehydes occupy an intermediate position between alcohols and carboxylic acids and can be easily oxidized to the latter or reduced to the former. In addition, aldehydes can form carbon–carbon bonds by aldolization reactions (α-aldolization for formaldehyde (11) and β-aldolization for those containing at least one hydrogen atom in the α position with respect to the carbonyl group (12, 13)). They can also lose oxygen in another carbon–carbon bond reaction (reductive coupling or "metathesis") to form symmetric olefins in liquid–solid slurries (14, 15) or in gas–solid reactions on certain metal-oxide single crystals and powders (16–18). Ketones can also be formed from aldehydes, and two pathways for their formation are

[1] To whom correspondence should be addressed. Present address: Department of Chemical Engineering, University of Illinois, Urbana, IL 61801.

[2] Present address: Département de Chimie, Université de Dakar, Sénégal.

0021-9517/95 $12.00

known. The first is via a two step-reaction: oxidation to carboxylates on the surface of an oxide (usually a basic oxide (19–22)), followed by the coupling of two carboxylates to form one molecule of ketone and one molecule of CO_2, leaving intact the oxygen of the support. Examples of relevant chemistry include the formation of acetone from acetates, of divinylketone from acrylates, and of diethylketone from propionates on TiO_2 (001) single crystals (23, 24), the formation of acetone and diethyl ketone from acetaldehyde and propionaldehyde, respectively, on the surface of Cu/ZnO catalysts (25), and the formation of diethylketone from propionaldehyde on lanthanide oxides (26). The second pathway for ketone formation is through the reaction of an adsorbed acyl group, $RC{=}O$, with an alkyl group; the acyl is formed by the abstraction of a hydrogen atom from the aldehyde (27–29), while the alkyl is formed by the dissociation of the hydrocarbon chain from the carbonyl group. Acetone can thus be formed from acetaldehyde by the reaction of an acetyl ligand with an adsorbed CH_3 group.

In this work CeO_2 was used as a support. Its reducibility and basicity favor oxidation (20) and aldolization reactions (30). Ce (IV) cations on a stoichiometric surface can be reduced to Ce (III) cations by hydrogen (20, 31–33) and thus favor reduction reactions. Reduced CeO_2 was observed to be active for the cross-reductive-coupling reaction between acetaldehyde and benzaldehyde to form $C_6H_5CH{=}CHCH_3$ (1-phenyl propene) (18). It is also an active support for Pd in syngas conversion to methanol (34, 35), as well as for Pt and Rh in catalytic converters (36–38) where its relatively easy reduction allows an intrinsic stream of oxygen to regenerate the active metal (38). Acetaldehyde reactivity was also studied on Pd/CeO_2 (a reduced metal on metal-oxide surface) and Co/CeO_2 (a partially reduced metal on metal-oxide surface) and on Pd–Co/CeO_2 catalysts. The comparison between the activity of these catalysts provides insights into the effect of Pd on Co when deposited on CeO_2. It was previously observed that Pd assisted in the reduction of Co both without support (39) and when using CeO_2 as a support and that Co shifted the syngas reaction products from methanol on Pd/CeO_2 to a mixture of methanol and ethanol on Pd–Co/CeO_2, although syngas reaction products on Co alone on CeO_2 were nonoxygenated hydrocarbons (40). Moreover, it was also observed that the presence of the two metals together on CeO_2 created more sites (40) for CO adsorption than could be accounted for by simply adding the number of sites for each metal taken alone. Thus, it is worth investigating the effect of adding Co (an inexpensive metal) to Pd (an expensive metal), in order to determine whether one can increase the conversion of acetaldehyde compared to Pd/CeO_2 alone. In addition, CeO_2 was also reported to undergo further reduction when loaded with noble metals, such as Rh and Pt (41, 42); this reduction might either activate or inhibit different acetaldehyde reactions.

In this study CeO_2, Pd/CeO_2, Co/CeO_2, and Pd–Co/CeO_2 catalysts were characterized by X-ray diffraction (XRD), X-ray photoelectron spectroscopy (XPS), and chemisorption (O_2 and CO), while the reactions of acetaldehyde were examined by temperature programmed desorption (TPD), and the adsorbed species were followed by infrared spectroscopy (FT-IR).

EXPERIMENTAL

1. Catalyst Preparation

Cerium oxide was precipitated from a solution of cerium nitrate (Fluka) at pH 8 using ammonia. After filtration, washing, and drying (for ca. 5 h at 400 K) it was calcined for ca. 5 h at 673 K under air. Pd/CeO_2 (3 wt%) was prepared by impregnating CeO_2 with a solution of 1 *M* HCl containing Pd ions (ex $PdCl_2$) and heated, while stirring, until paste formation. The catalyst was then dried and calcined as above. Co/CeO_2 (3 wt%) was prepared by impregnating CeO_2 with a solution of Co nitrate (Fluka) following the same procedure as for Pd/CeO_2. Pd (3 wt%)–Co/CeO_2 (3 wt%) was prepared by coimpregnating a solution of cobalt nitrate and $PdCl_2$ (1 *M* HCl) with CeO_2 followed by drying and calcination as above. Surface areas of these catalysts are presented in Table 1.

2. Chemisorption

A conventional U-shape quartz reactor and flow system were used. For each catalyst, 500 mg, was first recalcined under pure oxygen at 773 K (3 h) and then reduced by hydrogen overnight at 673 K (or 873 K in a few cases). After the catalyst was cooled under hydrogen to room temperature, He (ultrapure) (10 ml/min) was used to replace hydrogen for 30 min before sending oxygen pulses (1.10 ml per pulse) through the reactor. Thermal conductivity detectors (TCD) (HNU 320) connected to a Spectra Physics Chrom Jet integrator were used to follow adsorption, and a type-K thermocouple inside the reactor was used to monitor the temperature rise resulting from oxygen adsorption. Carbon monoxide chemisorption was performed in the same way as oxygen chemisorption.

3. X-Ray Diffraction

Catalysts were grounded to a fine powder before packing into the XRD sample holder. The XRD operating conditions were as follows. A Cu tube (broad focus) ($K\alpha$; λ = 1.514 Å) at 45 kV and 30 mA, an autodiverge slit, and a 0.2 mm receiving slit (no scatter slit) were used. The angle scanned was from 17 to 127 2θ. The Joint Committee of Powder Diffraction Data Service (JCPDS) was used to identify the patterns. Particle diameters were cal-

culated from the Scherrer equation (43) using the 111, 200, 220, and 311 diffraction lines of CeO_2 (44).

4. X-Ray Photoelectron Spectroscopy

XPS analyses were performed using a Perkin Elmer Physical Electronics Model 530 with a base pressure in the low 10^{-8} Torr range. Unreduced samples were loaded into the chamber without further manipulation. Prereduced samples were loaded onto the sample holder in a glove box compartment which was evacuated at 10^{-3} Torr and then backfilled with nitrogen (ultrapure). The sample holder consisted of a Perkin Elmer transfer vessel designed to maintain the integrity of the sample. The introduction chamber was first evacuated at 10^{-6} Torr before the transfer vessel was opened and the sample was loaded into the chamber. Mg$K\alpha$ X-ray irradiation was used at 300 W. Sample charging up to 3–4 eV occurred under X-ray irradiation. Binding energies were calibrated with respect to the signal for adventitious carbon (binding energy = 284.5 eV).

5. Temperature Programmed Desorption after Acetaldehyde Adsorption

TPD experiments were performed using the reactor–mass spectrometer system described previously (12). This apparatus consisted of the following: a tubular quartz reactor (diameter, 1 cm), thermal conductivity detector to measure the desorption signal, two roughing pumps, one diffusion pump (base pressure, 10^{-7} Torr), and a quadrupole mass spectrometer multiplexed with an IBM PC for data acquisition and data manipulation routines. All connections were made from heated 1/8-inch stainless steel tubes, and gases were controlled by mass flow meters. All catalysts were reduced in flowing hydrogen at 573 K overnight. After cooling at room temperature under hydrogen, hydrogen was displaced by purging with He (Matheson, ultrapure) for 1 h. Acetaldehyde was introduced (from a saturator; partial pressure, ca. 50 Torr)) in He flow (30 ml/min). Saturation uptake of the catalysts was determined by monitoring the mass spectrometer signal at m/e 29 (the most intense fragment of acetaldehyde). A decrease of the signal due to acetaldehyde adsorption on the catalyst followed by signal restoration was indicative of saturation of the surface. The total time for acetaldehyde adsorption was between 1 and 3 min, depending on the catalyst. Gaseous and reversibly adsorbed acetaldehyde were removed by purging with He for about 1 h. TPD was then started at a heating rate of 15 K/min from room temperature to 850 K. Up to 70 masses between 2 to 100 amu were monitored using the quadrupole mass spectrometer with a sampling period for the entire mass cycle of about 5 s. The pressure at the quadrupole during TPD was maintained at $0.9–1.0 \times 10^{-5}$ Torr.

Products were analyzed by their fragmentation patterns by the method described previously (12). This involved: (i) separating the peaks into different domains of temperature, (ii) analyzing the fragmentation patter of each product separately (by introducing it, if necessary, into the mass spectrometer in separate experiments) and calculating the mass spectrometer sensitivity factor relative to CO for each one using the method of Ko *et al.* (45), and (iii) starting from the most intense fragment for each product (such as m/e 29 for acetaldehyde) and subtracting the corresponding amounts of its other fragments until all signals were accounted for. The sensitivity factors of the different products observed during TPD are presented in Table 4. Yields reported represent the fraction of the total carbon desorbed contained in each species,

$$Y_i = \mathrm{PA}_i \times \mathrm{CF}_i \times \mathrm{Cn}_i / \sum_j \mathrm{PA}_j \times \mathrm{CF}_j \times \mathrm{Cn}_j,$$

where PA stands for peak area, CF, for correction factor; and Cn for number of carbon atoms per molecule, $j = i, \ldots, n$. The product selectivity (%) is

$$Y_i \times 100/(1 - Y_{\text{acetaldehyde}}).$$

6. Infrared Spectroscopy

IR studies were performed using a Nicolet 5DXC at a resolution of 4 cm^{-1}, and a number of scans per spectrum of 50. Self-supporting discs with a diameter of 13 mm were reduced overnight at 673 K, evacuated at 10^{-5} Torr, and cooled to room temperature before acetaldehyde adsorption. IR bands for acetaldehyde and adsorbed intermediates and products were assigned by comparison with literature values (see below) as well as with spectra obtained for adsorbates derived from CD_3CDO, CH_3COOH, and $CH_3CH{=}CHCHO$. Depending on the techniques used (IR, HREELS, and Raman) in previous studies on supported metals or single crystals, bands characteristic of acetaldehyde exhibit slight differences but are typically assigned as follows: ν_{as} (CH_3) at 3001–2990 cm^{-1}, ν_s (CH_3) at 2920–2917 cm^{-1}, ν (CH) at 2751–2745 cm^{-1}, ν (C=O) at 1722–1714 cm^{-1}, δ (CH_3) at 1431, 1426–1422 cm^{-1}, δ (C–H) at 1391–1389 cm^{-1}, and ν (C–C) at 1109 cm^{-1} (46). Acetaldehyde adsorption on the catalyst samples in this study was carried out at pressures between 0.25 and 1.2 Torr. In experiments where several spectra were collected as a function of temperature, the first set was collected after adsorption and evacuation at room temperature, then the catalyst was heated to the desired temperature and cooled to room temperature before further data acquisition.

TABLE 1

Surface Areas and Particle Diameters of Catalysts Used in This Study

Catalyst	Surface area (m^2/g catal) (from BET method)	Mean particle diameter (Å) (from XRD)
CeO_2	53	96
3 wt% Pd/CeO_2	54	91
3 wt% Co/CeO_2	20	84
3 wt% Pd–3 wt% Co/CeO_2	16	98

RESULTS

I. Characterization

1. BET, XRD, and O_2 Chemisorption

Table 1 presents the surface areas and mean particle diameters of CeO_2 and CeO_2-supported catalysts. While no difference in surface area was observed between Pd/CeO_2 and CeO_2 alone, impregnation of Co or Pd + Co decreased the surface area by a factor of 2 to 3. In contrast, no appreciable difference was observed for the mean particle dimensions calculated from the 111, 200, 220, and 311 diffraction lines of CeO_2 (44) using the Scherrer equation. It should be mentioned that the fluorite structure of CeO_2 was maintained for all catalysts and that no lines were observed related to Pd or Co compounds. It is unlikely that the drop in surface areas in the case of Co/CeO_2 and Pd–Co/CeO_2 is due to formation of new phases. It is tempting to attribute the drop in surface area to blocking of the micropores of the support by clusters of Co compounds or to a side reaction between nitrates (Co was deposited ex-nitrate) and Ce hydroxides during impregnation. This observation of decreased surface area, although not understood, was not investigated further in this work. CeO_2 reduced at 673 K chemisorbed 2.6×10^{20} [O] per gram or 4.9×10^{14} [O] per cm^2. Increasing the reduction temperature to 873 K decreased the BET surface area to 12 m^2/g but dramatically increased the oxygen uptake to 5×10^{15} [O] per cm^2.

2. X-Ray Photoelectron Spectroscopy (XPS)

All catalysts were analyzed by XPS. The Pd (3*d*), Co (2*p*), Ce (3*d*), O(1*s*), and C(1*s*) regions were investigated. All catalysts, both reduced and unreduced, contained nonnegligible amounts of surface carbon; in addition it appeared that the carbon concentration increased for reduced catalysts, probably through carbon diffusion from the bulk to the surface. No attempt was made to study in detail the different surface carbon species of each catalyst, but as an example, Fig. 1 presents carbon species on the surface of unreduced and reduced CeO_2. On the unreduced CeO_2 three peaks were present. They can be attributed to graphitic carbon, carbidic carbon, and carboxylate (and/or carbonate) species (21, 23) at about 283.0, 284.5–285, and 290–291 eV, respectively (Fig. 1A). On reduced CeO_2 the peak at about 284.5 eV increased in intensity while that attributed to oxygenated species, such as carboxylates (or carbonates), around 290 eV, decreased dramatically. It is likely that hydrogen reduction was responsible for this decrease. This result is rather important for the quantitative study of acetaldehyde TPD, since it indicates that, except for carboneous species not removed by calcination or by reduction at 673 K (species not likely to be removed during acetaldehyde TPD either), only minor amounts of oxygen-containing species were present.

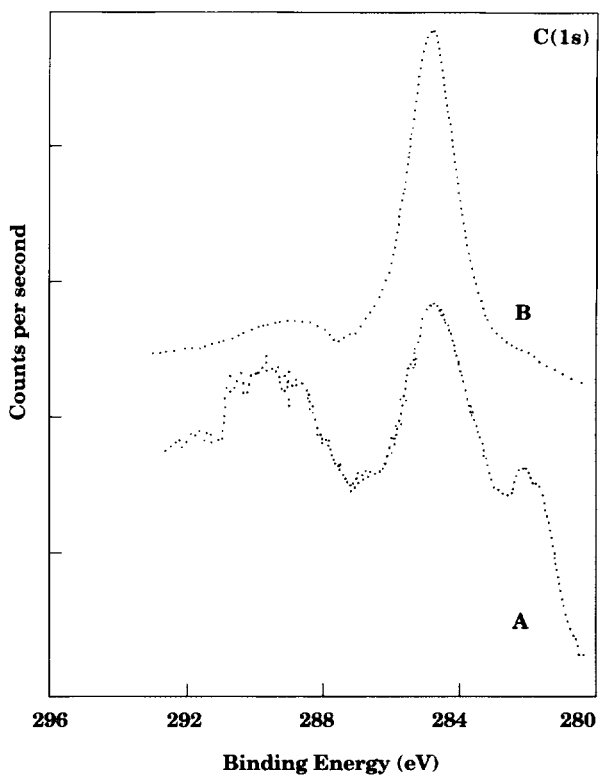

FIG. 1. C(1*s*) XPS of (A) unreduced CeO_2 and (B) reduced CeO_2.

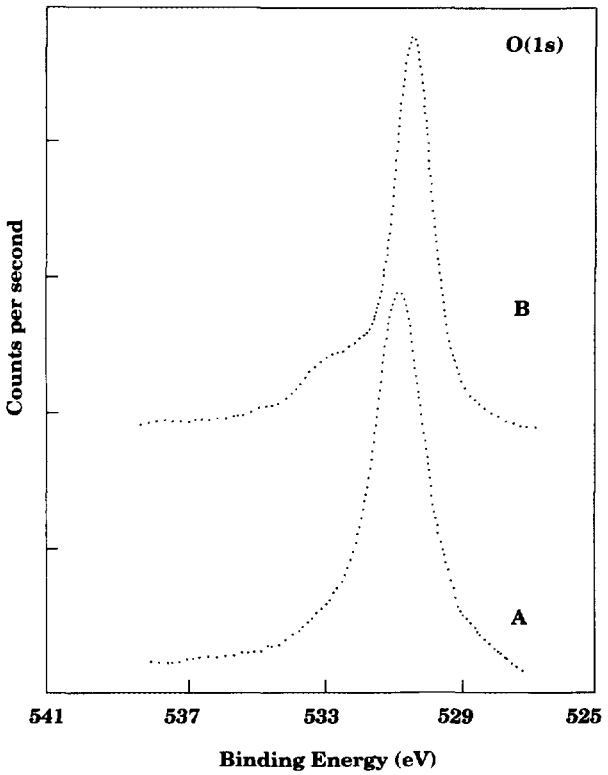

FIG. 2. O(1*s*) XPS of (A) unreduced CeO_2 and (B) reduced CeO_2.

Figure 2 presents the O(1*s*) spectra of CeO_2 before and after reduction. It should be noted that the other catalysts exhibited similar characteristics in the O(1*s*) region. Unreduced CeO_2 had a peak centered at 531 eV with a FWHM of 2.0 eV (Fig. 2A). The tail at higher binding energies and the large FWHM indicated the presence of several oxygenated species, in accord with the C(1*s*) spectrum of Fig. 1A. In contrast, reduced CeO_2 had a very narrow peak centered at 530.2 eV with a FWHM of 1.1 eV. Another peak, however, was observed at about 533 eV, most likely due to surface hydroxyls (47). The presence of a hydroxyl peak on reduced surfaces of metal oxides was previously observed on reduced TiO_2 single crystals (23, 48), reduced cobalt oxides (39), and reduced CeO_2 (49), among others.

Figure 3 presents the XPS Ce(3*d*) region. The unreduced CeO_2 showed a complex spectrum identical to that reported for fully oxidized CeO_2 by several workers (33, 50–61). The presence of the peaks identified as V, U, V″, U″, and V‴, U‴ is clearly noted. Figure 3B shows the Ce(3*d*) region of CeO_2 which had been reduced at 673 K (2 h at 1 atm hydrogen, 20 ml/min g catal.). The presence of V′ (885.0 eV) and U′ (903.7 eV) peaks clearly indicated that part of the Ce^{4+} was reduced to Ce^{3+}. The reduction of Ce cations of CeO_2 from 4+ to 3+ is in agreement with the results of several workers who studied the hydrogen-, Ar^+ sputtering-, or X-ray-induced reduction of CeO_2 alone (51–55, 57) or doped with other metals (60, 62) or other oxides (31, 51, 56). In summary, the surface of reduced CeO_2 was relatively free of oxygenated organic species, as demonstrated by its C(1*s*) spectrum, and contained Ce cations in the 3+ oxidation state in addition to Ce^{4+} cations (as demonstrated by the Ce(3*d*) spectrum).

Pd(3*d*) XPS clearly indicated the reduction of Pd cations to Pd metal (not shown). It should be noted that Pd metal was observed when Pd^{2+}, deposited on several oxides (ZnO (62), Al_2O_3 (63), TiO_2, CeO_2, Nb_2O_5 (64)), was reduced by hydrogen. Figure 4 presents the Co(2*p*) XPS of 3 wt% Co/CeO_2 after reduction with hydrogen at 673 K. The Co(2*p*) signal is complex (39), mainly because of two reasons: satellites of the main peak are present when Co atoms are in the paramagnetic state (39, 65–67) and because of the inverse shift of the Co^{2+} and Co^{3+} main peak positions, or in other words, the binding energy of Co^{2+} is higher than that of the Co^{3+} cations (68, 69). The presence of Co^{2+} is clear and evidenced as follows. Four peaks are present and are very similar to those of CoO spectra published by other workers (39, 69, 70). Co $2p_{3/2}$ at 781.0 eV and Co $2p_{1/2}$ lines at 797.0 eV were observed; the spin splitting of 16 eV was very close to that reported by others (68–70); the satellites at about 788 and 804 eV are those of the Co $2p_{3/2}$ and Co $2p_{1/2}$ lines,

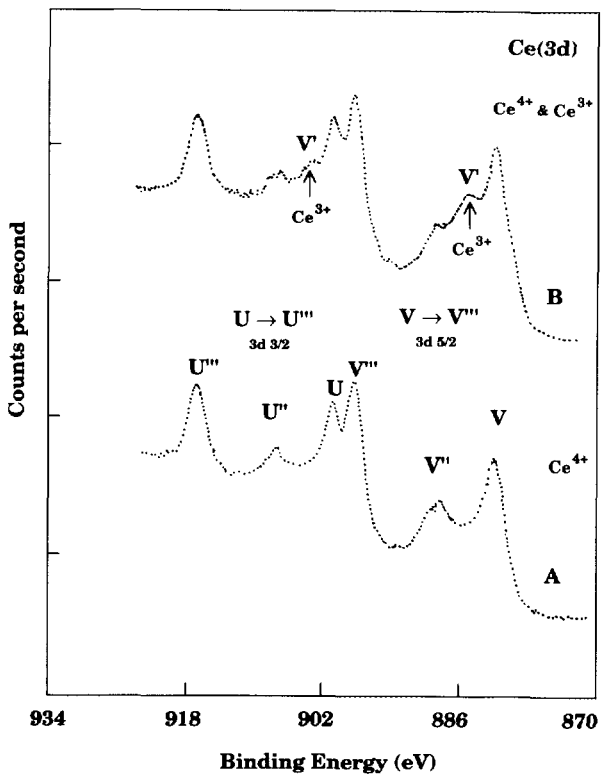

FIG. 3. Ce(3*d*) XPS of (A) unreduced CeO_2 and (B) reduced CeO_2.

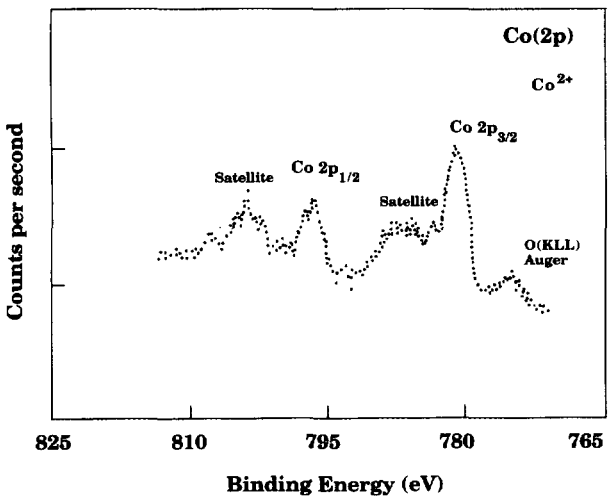

FIG. 4. Co(2p) XPS of reduced 3 wt% Co/CeO_2.

respectively. The important point to note is that Co(2p) XPS of Co^{3+} was shown to exhibit negligible satellite signals (69, 70), and a method of discriminating between Co^{2+} and Co^{3+} taking into consideration the presence or absence of satellites was previously presented in that work. Thus, the presence of these satellites unambiguously indicated the presence of Co^{2+}. Because the difference in binding energy between Co^{2+} and Co^{3+} is only about 1 eV and since the FWHM of the peak at 781.0 eV in Fig. 4 is about 3.0 eV, one cannot rule out the presence of Co^{3+} which should be at about 780.0 eV. A similar spectrum was observed for the Co(2p) signal for the $Pd–Co/CeO_2$ catalyst (not shown). Thus on both catalysts Co^{3+} was partially reduced to Co^{2+} with hydrogen at 673 K on CeO_2. There was no indication of a signal for Co metal which should exhibit a Co(2p) line at about 778 eV (70).

Atomic percentage concentrations at the surface of each catalyst were calculated from the XPS data for the reduced samples. There were no noticeable quantitative differences between the reduced and unreduced surfaces of all catalysts; the results for reduced catalysts are presented in Table 2. The relative atomic sensitivity factors (determined from experimental measurements of the corresponding pure compounds) used were as follows: Ce(3d) × 10, O(1s) × 0.66, Pd(3d) × 4.6, Co(2p) × 3.8. These values are very close to those calculated from the photoionization cross section data (39). Several points are important to mention. First, for all catalysts about 75% of the surface was composed of oxygen. The metal (Pd, Co, Pd–Co) to Ce atomic ratio of the surface and near surface was not equal to that theoretically expected, shown in parentheses in Table 2. However, the Co/Pd ratio for the 3 wt% Pd–3 wt% Co/CeO_2 catalysts was almost equal to unity (2.6/2.5). The high surface and bulk (and subsurface) concentration of the deposited metals compared to that theoretically "calculated" for both unreduced and reduced samples requires the following two comments: (i) Pd, Co, and Pd–Co were deposited from their precursor, on the surface of CeO_2, by impregnation followed by calcination at 673 K (5 h); thus it appears that calcination at this temperature (with metal loading of 3 wt%) does not assure homogeneous atomic distribution between the surface and bulk. It has been reported that for 0.8% Pt/SiO_2 the calculated and observed (by XPS and H_2 chemisorption) Pt to Si ratios are similar, while for 3.7% Pt/SiO_2 the observed ratio is three to four times higher than that calculated (72). Cluster formation (aggregation) of the dopants on the surface of the oxide is favored at high concentration. (ii) The unnoticeable difference of the surface and subsurface atomic concentration between the unreduced and reduced samples indicates that the extent of hydrogen reduction at 673 K is insufficient for "strong metal support interactions" (SMSI); in the SMSI regime a decrease in the atomic surface concentration of the metal would be expected due to the migration (decoration) of the support on the metal clusters. As an example the Pt/Si ratio for 3.4% Pt/SiO_2 reduced at 673 K is equal to 0.106, while that obtained after reduction at 973 K decreases to 0.038 (73).

If one assumes that the measured compositions reflect a homogeneous distribution in the surface and the near-surface region, and that 1 cm^2 contains 1×10^{15} atoms, then there would be 4×10^{13} atoms of Pd/cm^2, 3.6×10^{13} atoms of Co/cm^2, and 5.1×10^{13} [Pd + Co] atoms/cm^2 on Pd/CeO_2, Co/CeO_2 and $Pd–Co/CeO_2$ catalysts, respectively. Table 3 presents the number of metal atoms per cm^2 of catalyst at the surface as well as the number of CO molecules adsorbed on the surface at room temperature on the same lot of catalysts. Three important points are noted. First, the ratio of Pd to CO is very close to unity (within experimental error) which indicates that the assumption of "one CO molecule adsorbed per one Pd site" is quantitatively very satisfactory for reduced (673 K) Pd/CeO_2 catalysts. Second, the ratio of CO to Co is

TABLE 2

Surface Compositions of Catalysts from XPS

Catalyst	Atom %				
	Ce	Pd	Co	O	(Pd + Co)/Ce
3 wt% Pd/CeO_2	22.3	4.0		73.7	0.18 (0.05)[a]
3 wt% Co/CeO_2	22.6		3.6	73.7	0.16 (0.09)[a]
3 wt% Pd–3 wt% Co/CeO_2	20.2	2.5	2.6	74.8	0.25 (0.14)[a]
CeO_2	23.3			76.7	

[a] Bulk ratio.

TABLE 3

Surface Metal Atom Density and CO Uptakes for CeO_2-Supported Catalysts

Catalyst	Surface metal atom density from XPS (atoms/cm²) Pd	Co	CO uptake at 300 K (molecules/cm²)	CO/M
3 wt% Pd/CeO_2	4×10^{13}		3.7×10^{13}	0.93
3 wt% Co/CeO_2		3.6×10^{13}	3.5×10^{13}	0.97
3 wt% Pd, 3 wt% Co/CeO_2	2.5×10^{13}	2.6×10^{13}	20×10^{13}	3.9

also very close to one. Third, the CO/M ratio increased dramatically (by about ×4) in the case where Co–Pd were both present.

II. Reactivity of Acetaldehyde

1. Temperature Programmed Desorption

A. TPD after acetaldehyde adsorption on CeO_2. Figure 5 and Table 5 present the desorption products resulting from acetaldehyde TPD. Different products desorbed in different temperature domains. Acetaldehyde (CH_3CHO; *m/e* 29) desorbed with a peak temperature of 390 K and represented more than half of the total products. Ethanol (CH_3CH_2OH; *m/e* 31, 45, and 46) desorbed in two peaks, the first at 390 K (a shoulder coincident with desorption of acetaldehyde) and the second at 470 K; together these peaks accounted for 6% of the acetaldehyde converted. Water desorbed in a broad spectrum (not shown) with maxima at ca. 520 K (a large peak) and ca. 750 K. Methane (*m/e* 15 and 16) and CO_2 desorbed at about 750 K, while CO desorbed at slightly higher temperature, 780 K. Higher molecular weight products containing more than two carbon atoms were also observed. Acetone (CH_3COCH_3; *m/e* 58 and 43) desorbed at 620 K (selectivity 12%), and butadiene ($CH_2{=}CHCH{=}CH_2$; *m/e* 54, 53, and 39) at 570 K, while 2-butene ($CH_3CH{=}CHCH_3$; *m/e* 56) desorbed in two peaks, one at 560 K and one broad peak at ca. 650 K. Butene and butadiene were most likely formed by reductive coupling of acetaldehyde. In addition, products of β-aldolization of acetal-

TABLE 4

Mass Spectrometer Correction Factors and Major Fragments of Products Resulting from Acetaldehyde–TPD

Products	Correction factor (for fragments shown in bold)	Major fragments
Methane	3.7	**16**, 15
Ethylene	2	**28**, 27, 26
Acetaldehyde	3	**29**, 44
Ethanol	2.1	**31**, 45, 46
Propane	2.2	29, 28, 44, 41, **39**
CO_2	1.5	**44**
Butadiene	3.8	**54**, 53, 39
Butene	2.5	**56**, 55, 41
Acetone	9	**58**, 43, 15
Crotonaldehyde	5.6	**70**, 69, 41
Crotyl alcohol	22	**72**, 55, 43, 29

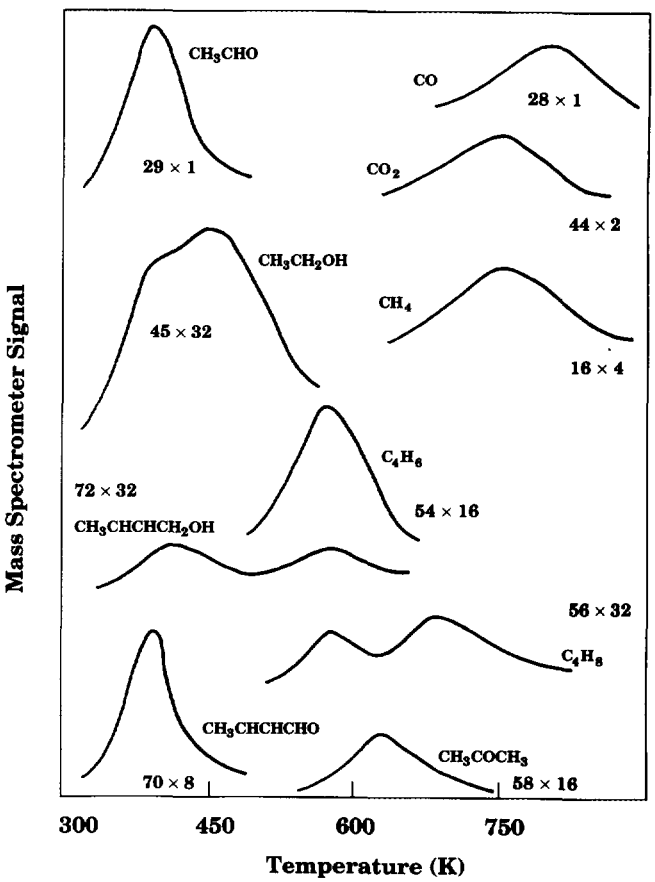

FIG. 5. Temperature-programmed desorption after acetaldehyde adsorption, at room temperature, on CeO_2.

TABLE 5

Fractional Yield (Carbon Basis) and Percentage Selectivity of Products Desorbing during Acetaldehyde–TPD on CeO_2

Product (principal fragment)	Peak temperature (K)	Fractional yield	Selectivity (%)
Acetaldehyde (29)	390	0.53	
Ethanol (45)	390, 450	0.03	6
Methane (16)	750	0.05	10
CO (28)	770	0.04	8
CO_2 (44)	750	0.02	4
Butadiene (54)	570	0.04	8
2-Butene (56)	570, 650	0.02	4
Acetone (58)	630	0.06	12
Crotonaldehyde (70)	390	0.13	28
Crotyl alcohol (72)	390, 570	0.09	20

dehyde were also observed: crotonaldehyde (CH_3CH=$CHCHO$; *m/e* 70, and 69) and crotyl alcohol (CH_3CH=$CHCH_2OH$; *m/e* 27, 55, and 72) desorbed at 390 K; together they accounted for 48% of the acetaldehyde converted.

B. TPD after acetaldehyde adsorption on metal-doped catalysts. B1. 3 wt% Pd/CeO_2. Figure 6 presents the products resulting from acetaldehyde TPD on 3 wt% Pd/CeO_2. Acetaldehyde desorbed at 390 K followed by ethanol at 400 K; only a single desorption peak for either product was observed. Acetone and propane desorbed simultaneously at 560 K. CO desorbed at 650 K, while CO_2 desorbed in two peaks, the first at 650 K, and the second at 800 K. Two characteristics distinguish these spectra from those obtained on CeO_2. First, propane was observed, most likely from total reduction of acetone by spillover of hydrogen provided by the presence of Pd (propane was previously observed as the major product from acetone on Cu/Zn catalysts (25)). Propane (MW 44) was clearly distinguished from acetaldehyde (MW 44) by its fragmentation pattern as follows: the intensity ratios for mass fragments 41/44 and 39/44 are 1 and 0.93, respectively, for propane, while those for acetaldehyde are 0.25 and 0, respectively. Second, the acetone desorption peak was 70 K lower than on CeO_2 and, as will be discussed later, this suggests that acetone formation on these two surfaces (CeO_2 and Pd/CeO_2) may follow two different routes. The absence of mass fragments corresponding to butene and butadiene indicates that addition of Pd to CeO_2 totally suppressed the reductive coupling of acetaldehyde to olefins. Crotonaldehyde was not observed, as evidenced by the absence of masses corresponding to its parent molecule (*m/e* 70). In contrast, small amounts of crotyl alcohol were produced as indicated by its desorption at ca. 550 K (*m/e* 72, 57, 55, and 27). The yields of the different products are presented in Table 6.

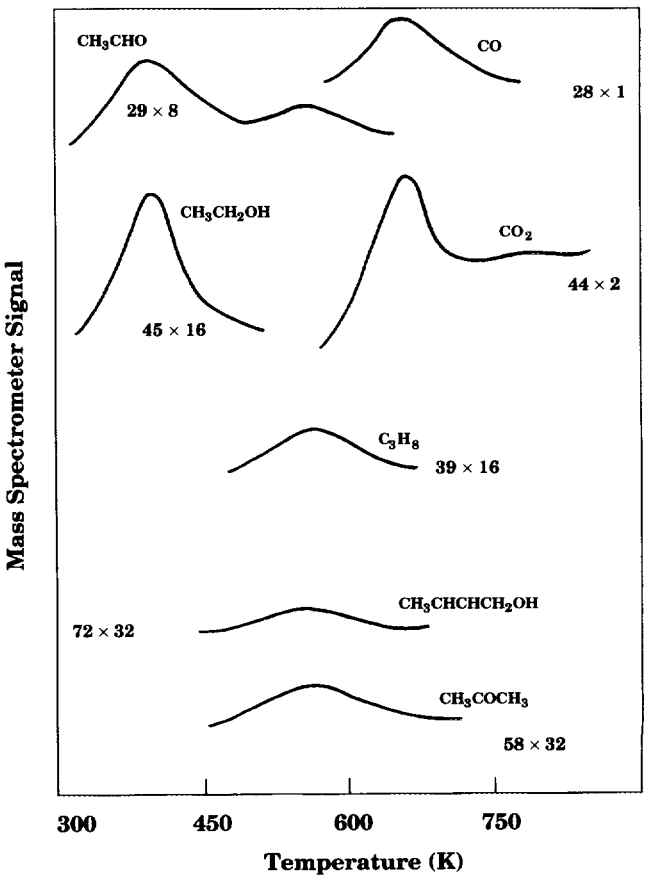

FIG. 6. Temperature-programmed desorption after acetaldehyde adsorption, at room temperature, on 3 wt% Pd/CeO_2.

About 76% of adsorbed acetaldehyde reacted during TPD. However, only 27% of that gave ethanol. The C_3 species, acetone and propane, accounted for 18% of the carbon contained in the products, CO_2 and CO for 46%. CO_2 and CO can be formed from acetate decomposition on CeO_2 (see IR results below). In the presence of Pd,

TABLE 6

Fractional Yield (Carbon Basis) and Selectivity of the Different Products Desorbing during Acetaldehyde–TPD on 3 wt% Pd/CeO_2

Product (principal fragment)	Peak temperature (K)	Fractional yield	Selectivity (%)
Acetaldehyde (29)	390	0.24	
Ethanol (45)	400	0.20	27
Propane (39)	560	0.10	13
Acetone (58)	560	0.04	5
CO (28)	650	0.18	23
CO_2 (44)	640, 800	0.18	23
Crotonaldehyde (70)	—		
Crotyl alcohol (72)	550	0.06	8

surface acetates did not undergo carboxylate coupling to acetone, but decomposed. It was previously observed that acetates, formed from acetic acid on Pd (111), decomposed to CO and CO_2 (72). The second desorption peak for CO_2 (5%) at 800 K is probably due to burnoff of surface carbon.

B2. 3 wt% Co/CeO_2. Figure 7 and Table 7 present the products desorbing during acetaldehyde TPD on Co/CeO_2. Unlike the case of acetaldehyde on Pd/CeO_2, ethanol desorbed in two peaks, one at 420 K and the second at 480 K. The peak shapes and desorption temperatures were very similar to those observed for acetaldehyde TPD from CeO_2 alone. The intensity of the first peak was about half that of the second, and both occurred but at slightly higher temperature than in the case of CeO_2. Acetaldehyde desorbed in a single peak at about 400 K as in the case of acetaldehyde/CeO_2 and acetaldehyde/Pd/CeO_2 TPD. Acetone desorbed in two peaks, a small one at 560 K and a larger one at 640 K. The first desorption resembled that observed on Pd/CeO_2. The second acetone peak was 100 K higher, falling in the region of acetone desorption from

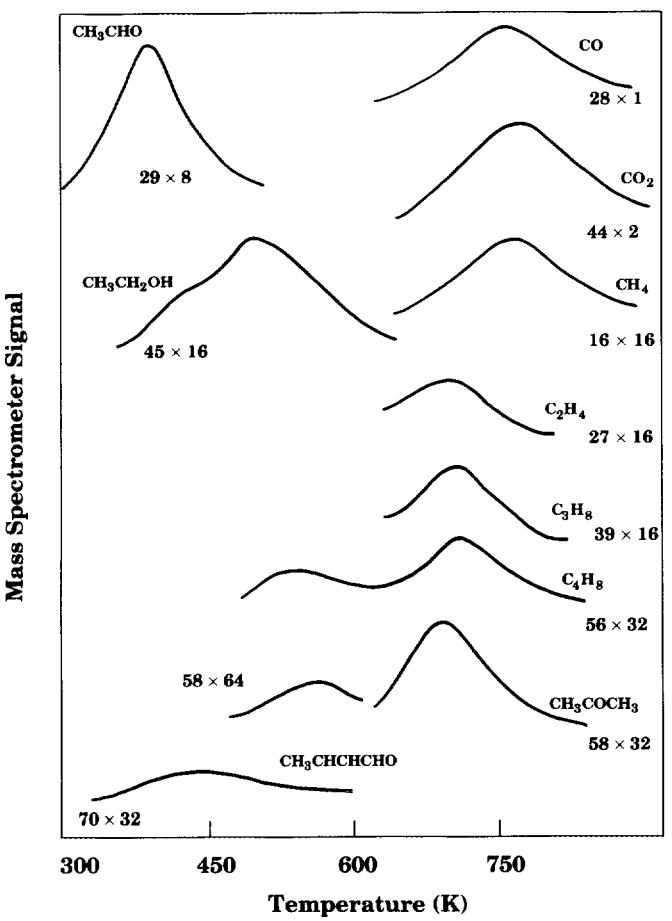

FIG. 7. Temperature-programmed desorption after acetaldehyde adsorption, at room temperature, on 3 wt% Co/CeO_2.

TABLE 7

Fractional Yield (Carbon Basis) and Selectivity of the Different Products Desorbing during Acetaldehyde–TPD on 3 wt% Co/CeO_2

Product (principal fragment)	Peak temperature (K)	Fractional yield	Selectivity (%)
Acetaldehyde (29)	390	0.34	
Ethanol (45)	420, 480	0.11	17
Methane (16)	750	0.03	4
Ethylene (27)	700	0.07	10
Propane (39)	700	0.13	20
Butene (56)	550, 770	0.02	4
Acetone (58)	560, 660	0.09	15
Crotonaldehyde (70)	420	0.02	4
CO (28)	750	0.09	13
CO_2 (44)	780	0.09	14

CeO_2. While aldolization did lead to formation of crotonaldehyde (*m/e* 70) which desorbed at 420 K, the yield of this product was one order of magnitude less than on CeO_2 alone (Fig. 5 and Table 5). Nonnegligible amounts of CO (13%) and CO_2 (14%) were also formed which desorbed at 750 K and 780 K, respectively. At 700 K ethylene and propane desorbed with selectivities of 10 and 20%, respectively. Small amounts of methane (*m/e* 16) and C_4 hydrocarbons (*m/e* 56) were also present.

B3. 3 wt% Pd–3 wt% Co/CeO_2. Figure 8 and Table 8 present the products desorbing during acetaldehyde TPD on $Pd–Co/CeO_2$. Almost complete reaction of acetaldehyde was observed (84% conversion). A complex product desorption spectrum was observed due to the presence of both metals together on ceria. Analysis of the products indicated patterns which can be related to Pd, others to Co, and others to the combined effect of both metals. Analysis of the product distribution from Fig. 8 gave the following. First, at 390 K only small amounts of acetaldehyde were observed. On CeO_2, Pd/CeO_2, and Co/CeO_2, acetaldehyde TPD also showed this desorption state. Only one peak for ethanol desorption was observed (at 410 K); this resembled that from Pd/CeO_2 in acetaldehyde TPD and was unlike that on Co/CeO_2 where two ethanol peaks were observed (at 420 K and 490 K, respectively). A plausible explanation for the influence of Pd on Co is that intimate contact exists between the two metals which results in a more facile reduction of Co. Previous TPR experiments indicated that Co was reduced in two peaks in Co/CeO_2 (at 445 K and 533 K), but only one relatively broad peak was observed when Pd was added to Co/CeO_2 (385–415 K) (40). At 450 K acetaldehyde desorbed from $Pd–Co/CeO_2$ accompanied by methane and ethylene. The production of methane and ethylene at this low temperature occurred only in the presence of both metals together on the surface of CeO_2 and was not

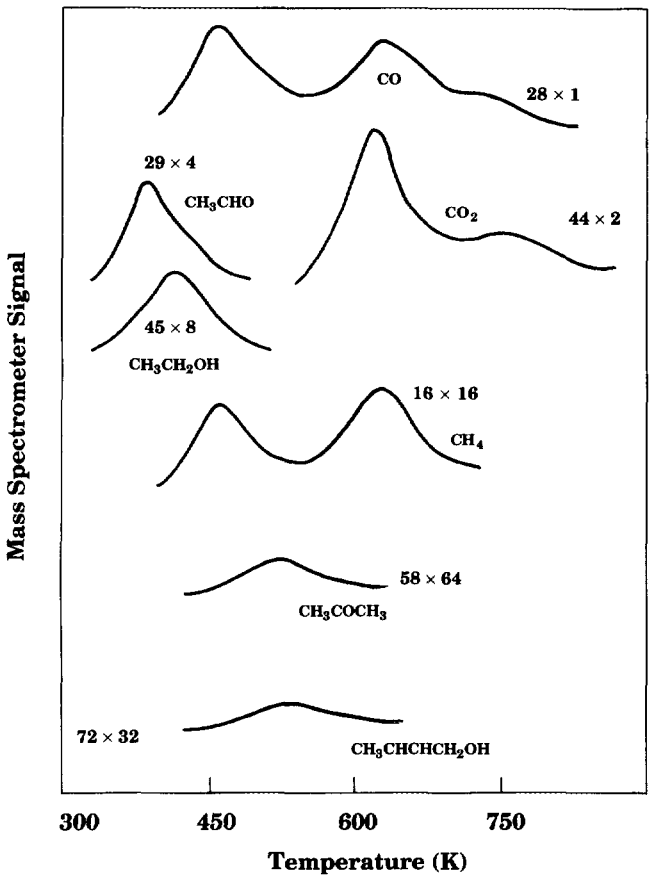

FIG. 8. Temperature-programmed desorption after acetaldehyde adsorption, at room temperature, on 3 wt% Pd, 3 wt% Co/CeO_2.

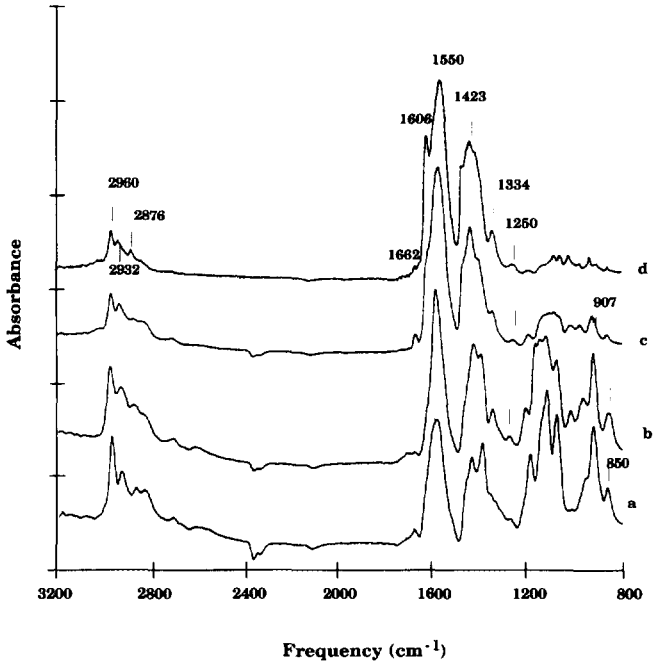

FIG. 9. IR spectra after acetaldehyde adsorption, at room temperature on CeO_2: (a) 0.15-Torr exposure at room temperature, after 2 min of evacuation (10^{-5} Torr); (b) after 20 min of evacuation (10^{-5} Torr); (c) surface in (b) heated to 393 K; (d) surface in (c) heated to 454 K.

observed on Pd/CeO_2 or on Co/CeO_2. At 520 K, peaks were observed corresponding to small amounts of acetone and crotyl alcohol (or butyraldehyde, it was not possible to distinguish between these two possible products in this case due to the small amounts desorbed). At 615 K methane desorbed, accompanied by CO at slightly higher temperature (630 K) and CO_2. Finally, at 730–750 K CO and CO_2 desorbed (acetaldehyde TPD from all the catalysts examined in this study gave rise to CO and CO_2 desorption within this temperature domain). No C_4 hydrocarbons were observed.

TABLE 8

Fractional Yield and Selectivity of the Different Products Desorbing during Acetaldehyde–TPD on 3 wt% Pd–3 wt% Co/CeO_2

Product (principal fragment)	Peak temperature (K)	Fractional yield	Selectivity (%)
Acetaldehyde (29)	390, 450	0.16	
Ethanol (45)	410	0.08	10
Methane (16)	450, 615	0.27	32
Ethylene (28)	450	0.06	7
CO (28)	450, 630, 730	0.17	20
CO_2 (44)	615, 750	0.19	23
Acetone (58)	520	0.02	2
Crotyl alcohol or butyraldehyde (72)	520	0.06	7

In order to follow the adsorbed species formed during acetaldehyde reactions on the surface, FT-IR spectra were obtained as a function of temperature on CeO_2, Pd/CeO_2, Co/CeO_2, $Pd–Co/CeO_2$ catalysts.

2. *Infrared Spectroscopy*

A. Acetaldehyde adsorption. Spectra a and b of Fig. 9 present IR bands obtained after acetaldehyde adsorption on reduced CeO_2 at room temperature and evacuation for (a) 2 and (b) 20 min. Several adsorbed species were identified. The bands at 2930 (ν_s CH), 1559 (ν_{as} COO), 1423 (ν_s COO), and 1334 cm^{-1} (δ CH) corresponded to acetates (73, 74). Those at 2965 (ν_{as} CH), 2870 (ν_s CH) 1376 (δ CH), 1067 (ν CO), and 875 cm^{-1} (ν CCO) corresponded to ethoxy species (75, 76). Thus, ethoxides and acetates were formed upon adsorption of acetaldehyde on the surface of reduced ceria at room temperature. Acetate formation from acetaldehyde (and carboxylates from aldehydes, in general) was previously observed on several oxides including ZnO (19, 77) and TiO_2 (12). Heat-

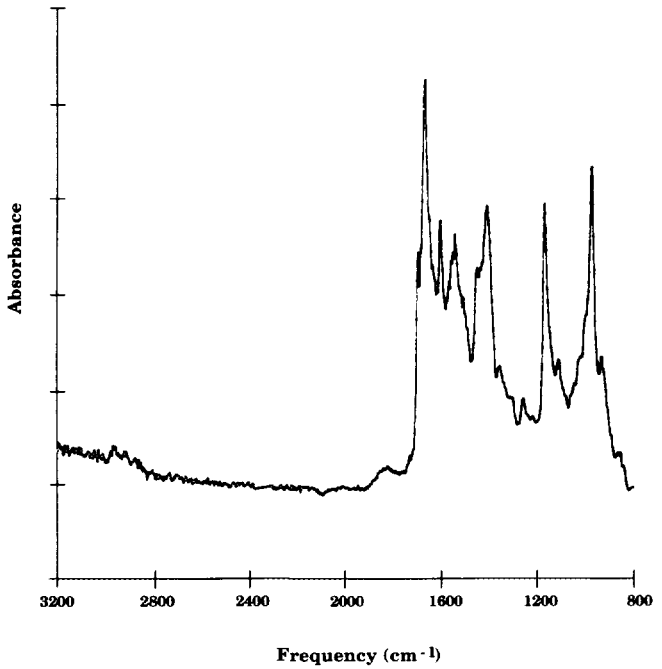

FIG. 10. IR spectra after adsorption of crotonaldehyde on the surface of 3 wt% Pd/CeO_2.

ing the surface to 390 K resulted in almost complete disappearance of ethoxide species and an increase of acetates. The dramatic decrease of ethoxide species is consistent with TPD results (Fig. 5) where ethanol desorbed with a peak temperature of 390 K. On CeO_2, it was reported (78) that acetaldehyde was reduced to ethanol and also reacted, via β-aldolization, to yield (after dehydration) crotonaldehyde. TPD experiments in this work also indicated the desorption of crotonaldehyde and crotyl alcohol (Table 5 and Fig. 5) at 390 K. In Fig. 9 IR bands at 1664–1660 and 1606 cm^{-1} are attributed to crotonaldehyde [in a separate experiment crotonaldehyde was adsorbed (Fig. 10) and bands at 2965, 2918, 1662, 1600, 1404, 1160, 1108, and 968 cm^{-1} were observed.] The band at 1662 cm^{-1} is attributed to ν CO while those at 1600, 1404, 1160, 1108, and 968 m^{-1} are attributed to (ν C=C), (δ CH), (ν CC, ρ CH_3), (ν CC), and (ρ CH_3), respectively. It was not possible to distinguish between crotonaldehyde and crotyl alcohol in the reaction of acetaldehyde on CeO_2 (Fig. 9) since the gas phase crotyl alcohol spectrum (not shown) also gave bands at 2925, 2875, 1690, 1125, 1090, and 975 cm^{-1} which were consistent with literature spectra (79). However, one can clearly rule out butyraldehyde since: (i) TPD spectra indicated the absence of mass fragments corresponding to butyraldehyde (the high yield of C_4 products permitted cracking pattern identification) and (ii) the gas phase spectrum of butyraldehyde (not shown) gave ν CO at 1750 cm^{-1} which was not observed in Fig. 9 (even taking into account the expected shift downward by 30 to 40 cm^{-1} for ν CO in the adsorbed state (82)).

B. Acetaldehyde adsorption on 3 wt% Pd/CeO_2. Unlike on CeO_2 alone, acetaldehyde multilayers were observed on 3% Pd/CeO_2 (Fig. 11) (2975, 1715, and 1451 cm^{-1}). The intensities of these bands decreased with heating; in addition, acetaldehyde decomposition gave adsorbed CO (2070, 1929, and 1864 cm^{-1}). CO formation was previously observed from acetaldehyde on supported metals; on Pt bands at 2030 and 2065 cm^{-1} were attributed to linear CO, and bands at 1850 and 1865 cm^{-1} were attributed to bridging CO (80); on Rh (111) bands at 2070 cm^{-1} (linear CO) and at 1850 cm^{-1} (bridging CO) were also reported following acetaldehyde adsorption (81). The band position of CO, observed also on Pt/CeO_2 (82), depends on the coverage and on dipole–dipole coupling of linear CO. On Pd/CeO_2 (Fig. 11) the band at 2070 cm^{-1} was attributed to linear CO, while those at 1929 and 1864 cm^{-1} were attributed to bridging CO. Two other bands were also observed at 1750 and 1730 cm^{-1} which will be discussed below.

Adsorption of acetic acid on this catalyst (Fig. 11c) gave bands at 1560–1540 cm^{-1} (ν_{as} COO), 1451 cm^{-1} (δ_{as} CH_3), 1400 cm^{-1} (ν_s COO), 1340 cm^{-1} (δ_s CH_3), and 1020 cm^{-1} (ρ CH_3). On Rh/CeO_2 (73) acetic acid gave bands at 1550, 1425, and 1325 cm^{-1} in addition to ν CH_3 bands at 2930 and 3000 cm^{-1}, while on Pd/Al_2O_3 adsorption of

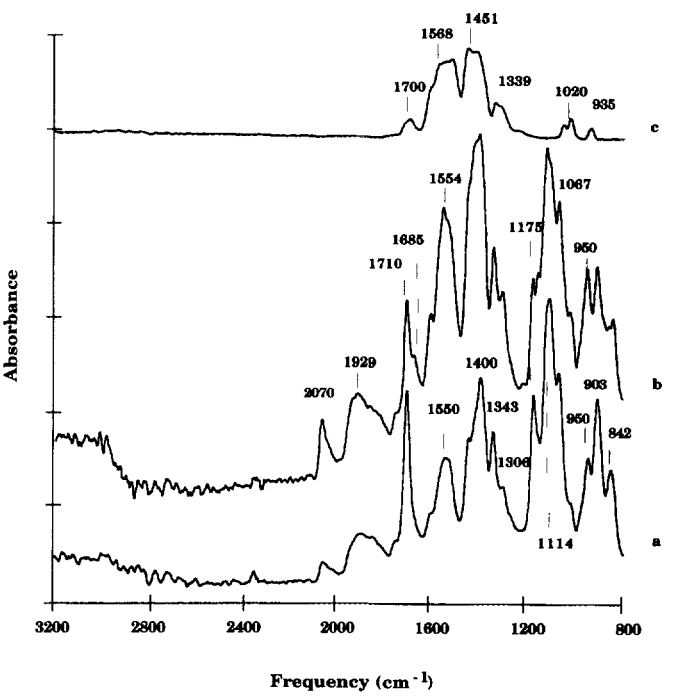

FIG. 11. IR spectra of 3 wt% Pd/CeO_2: (a) after acetaldehyde adsorption at room temperature (1.2 Torr); (b) surface in (a) heated to 335 K, (c) after acetic acid adsorption (1 Torr).

acetic acid gave bands at 2941, 1579, 1468, 1396, and 1334 cm^{-1} (74). The presence of these bands (1555–1535, 1451, 1400, 1343, and 1020 cm^{-1}) on Pd/CeO_2 from acetaldehyde at room temperature confirms the presence of acetate species, demonstrating the oxidation of part of the acetaldehyde (as was also observed on CeO_2 alone (Fig. 9)). Ethoxide species were identified following acetaldehyde adsorption at room temperature by their bands at 2979 (ν CH_3), 1400 (δ CH_3), 1114 (ρ CH_3, ν C–C), 1067 (ν C–O), and 842 cm^{-1} (ν_s CCO). This is in agreement with TPD results, where ethanol was formed from acetaldehyde and desorbed with a peak maximum at 400 K. Thus, one can confirm the oxidation and reduction of acetaldehyde on Pd/CeO_2 to acetates and ethoxides, respectively. The bands at 1220 (ν C=O), 1175 (ν CC), and 950 cm^{-1} (ρ CH_3) were attributed to η^2 (C, O) acetaldehyde, which may be the precursor, of ethoxide species, η^2 (C, O) acetaldehyde was previously observed from acetaldehyde and from ketene on Ru (001) (83, 84) and characterized by bands at 2755–2740 (ν CH), 1365 (δ CH_3), 1275 (ν CO), 1135–1105 (ν CC), and at 975 cm^{-1} (ρ CH_3). It was also reported that the decomposition of these species yielded CO (84).

Unlike the case of CeO_2 alone, bands corresponding to crotonaldehyde or crotyl alcohol were not observed on Pd/CeO_2. This is in agreement with TPD results where only traces of crotyl alcohol desorbed (Fig. 6). In fact this is most likely due to the effect of further reduction of the support by Pd. The effect of reduction of CeO_2 by the presence of the noble metal was previously observed on Rh/CeO_2 (41), and on $Pd/CeO_2/Al_2O_3$ (31). It was mentioned that the presence of highly dispersed Rh resulted in almost complete reduction, with hydrogen, of the surface Ce IV to Ce III cations (41). In order to follow the effect of reduction of the support in the presence of Pd, acetaldehyde was adsorbed on 3 wt% Pd/CeO_2 catalyst previously reduced at 433 K. Figure 12 presents the region between 1650 and 1765 cm^{-1} of the IR spectra after adsorption of acetaldehyde. While crotonaldehyde was not formed when the catalyst was reduced at 673 K (shown by the absence of the band at 1662 cm^{-1} in Fig. 12A,1) a small peak at 1662 cm^{-1} was observed when the reduction was performed at 433 K, indicating the presence of crotonaldehyde (Fig. 12A,2 and 3).

The unique characteristic of acetaldehyde adsorption on Pd/CeO_2 is the presence of the band at 1685 cm^{-1}. This band was very weak at room temperature (Fig. 12A,1) but was clearly present at 335 K (Fig. 12A,2); this band was not observed on CeO_2 alone (Fig. 9). It shifted to 1667 cm^{-1} when CD_3CDO was used instead of CH_3CHO (not shown). This same band was observed on sodium-doped Pt/SiO_2 at 1684 cm^{-1} (85) (but was absent on nondoped Pt/SiO_2) and was attributed to acetyl species, $CH_3C{=}O$. On Pt and Pd acetyls were identified by their ν CO mode

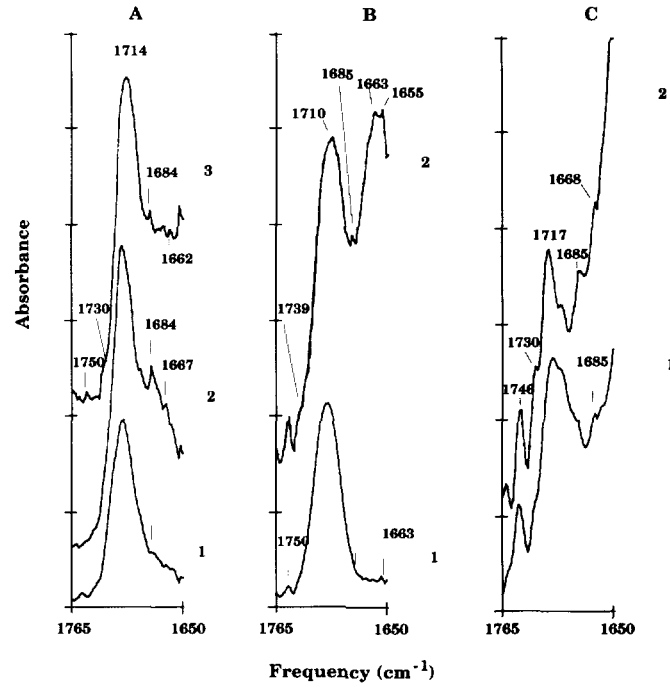

FIG. 12. IR spectra after acetaldehyde adsorption. (A) 3 wt% Pd/CeO_2: 1, room temperature (catalyst reduced with hydrogen at 673 K); 2, surface in 1 heated to 335 K; 3, 373 K (catalyst reduced with hydrogen at 433 K). (B) 3 wt% Co/CeO_2: 1, 1.5 Torr at room temperature; 2, surface in 1 heated to 335 K. (C) 3 wt% Pd–3 wt% Co/CeO_2: 1, 2.5 Torr at room temperature; 2, surface in 1 heated to 335 K.

at 1650 and 1667 cm^{-1}, respectively (83, 86); on Pd (111) acetyls derived from acetaldehyde exhibited a ν CO band at 1565 cm^{-1} (87) and those from ethanol at 1585 cm^{-1} (88), and on Pt (111) a band at 1600 cm^{-1} was attributed acetyl species derived from ketene (83). Other organometallic complexes incorporating acetyl species have characteristic bands in the same region; examples include $PtBr(COCH_3)$ at 1630 cm^{-1} (89), $Re(CO)_5(COCH_3)$ at 1617 cm^{-1} (90), and $Cp_2Ti(COCH_3)(Cl)$ at 1620 cm^{-1} (91). Acetaldehyde TPD on Pd/CeO_2 (Table 6) indicated that acetone desorbed at 560 K together with propane; this was 70 K lower than acetone formation from acetaldehyde on CeO_2 alone. Acetone formed on Pd/CeO_2 most likely occurs through reaction of an adsorbed acetyl (CH_3CO (a)) with adsorbed methyl (CH_3 (a)); CH_3 species are formed by decarbonylation of a portion of the adsorbed acetaldehyde. The band at 1685 cm^{-1} on Pd/CeO_2 attributed to acetyl species is consistent with this suggestion.

C. Acetaldehyde adsorption on 3 wt% Co/CeO₂. At room temperature on Co/CeO_2, like Pd/CeO_2 and unlike CeO_2, molecular acetaldehyde was observed (bands at 1712 and 2975 cm^{-1}, Fig. 13). The comparison between this spectrum and that of Pd/CeO_2 (Fig. 11) indicated that (i) unlike the case of Pd/CeO_2, neither linear nor bridging

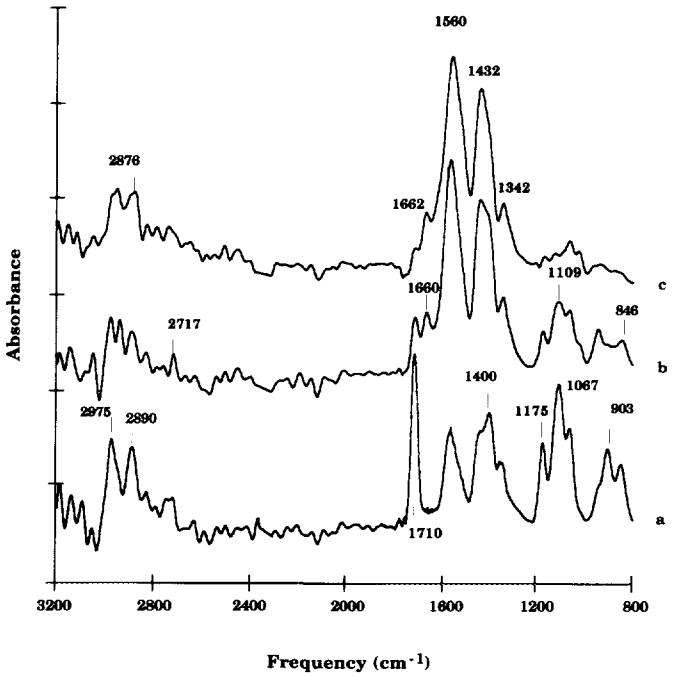

FIG. 13. IR spectra after adsorption of acetaldehyde on the surface of 3 wt% Co/CeO_2: (a) at room temperature; (b) surface in (a) heated to 335 K; (c) surface in (b) heated to 395 K.

CO was observed, as evidenced by the absence of bands at 2070, 1929, and 1864 cm^{-1}; (ii) as on Pd/CeO_2, bands at 1750 and 1739 cm^{-1} were present following acetaldehyde adsorption (these bands will be discussed later); and (iii) as on Pd/CeO_2 (Fig. 11) and CeO_2 (Fig. 9), acetates were present, as evidenced by the bands at 1560, 1432, and 1348 cm^{-1}. Ethoxide species were also present, especially at room temperature, as demonstrated by bands at 1067 and 1109 cm^{-1}. Crotonaldehyde was present, in very small amounts at room temperature (Fig. 12B,1) but in considerable amounts at 335 K (Fig. 12B,2). Since Co/CeO_2 was reduced at 673 K prior to acetaldehyde adsorption and since Pd/CeO_2 reduced at this temperature did not show evidence for crotonaldehyde in either IR or TPD experiments, one can argue that the effect of Co as a reducing agent for CeO_2 in presence of hydrogen is less dramatic than that of Pd. Acetyl species were only present, as a small band at 1684 cm^{-1}, when the surface was heated to 335 K. If one attributes the low temperature desorption of acetone to the reaction of an acetyl with an adsorbed methyl, the IR and TPD results are then in agreement for this catalyst. Two peaks for acetone were observed, one at 560 K (at the same temperature of acetone produced from acetyles on Pd/CeO_2 (Fig. 6)) and one at 660 K (in the same region of acetone desorption on CeO_2 (Fig. 5)). These results support the suggestion of two sources for acetone formation: one due to the acetyl on the metal (Pd or Co) and one due to acetate ketonization on the support. Also as for Pd/CeO_2, η^2 (C, O) acetaldehyde was present in the IR spectrum at room temperature, fingerprinted by a band at 1175 cm^{-1}.

D. Acetaldehyde adsorption on 3 wt% Pd–3 wt% Co/CeO_2. Molecular acetaldehyde gave rise to weak bands at 1718–1720 cm^{-1} on Pd–Co/CeO_2 (Figs. 14 and 12C). Acetate species were also present. Acetic acid adsorption gave bands at 1554, 1456, 1428, 1338, 1048, 1020, and 935 cm^{-1} (Fig. 14c); the comparison between this spectrum and that after adsorption of acetaldehyde at room temperature (Fig. 14a) clearly identified acetate species. Ethoxide species were also present, as shown by bands at 1109 and 1053 cm^{-1}. Thus, as on all the other catalysts, part of the acetaldehyde was reduced to ethoxides and another part was oxidized to acetates. η^2 (C, O) acetaldehyde was also observed with peaks at 1268, 1156, and 940 cm^{-1} (compared to 1220, 1175, and 950 cm^{-1} for Pd/CeO_2). Acetyl species were identified by the band at 1685 cm^{-1} (Fig. 12C,1 and 2). If one compares these results to the corresonding TPD spectrum (Fig. 9) one is led to the following conclusions. The small peak for acetone at 520 K during acetaldehyde TPD is again likely due to the reaction of an acetyl with an adsorbed methyl species. Acetates were also observed by IR on this catalyst; however, the absence of acetone desorption at high temperature indicated that acetates did not undergo ketonization

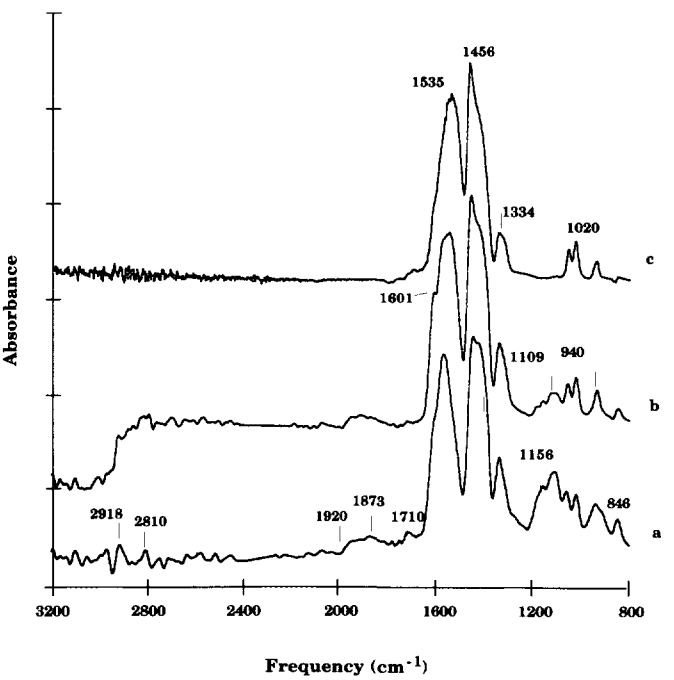

FIG. 14. IR spectra after adsorption of acetaldehyde on the surface of 3 wt% Pd–3 wt% Co/CeO_2: (a) 2.5 Torr at room temperature; (b) surface in (a) heated to 335 K; (c) after acetic acid (0.23 Torr) adsorption.

but instead decomposed directly to CH_4, CO, and CO_2. In this regard the Pd–Co catalyst is similar to Pd/CeO_2 rather than to Co/CeO_2. The aldolization reaction was a minor contributor to both TPD results and IR spectra; Fig. 12C,1 and 2, shows a weak band at 1668 cm^{-1}.

E. Assignment of bands around 1750 cm^{-1}. Bands at 1750, 1739, and 1730 cm^{-1} were observed (Fig. 12). On Rh/CeO_2 it was postulated that Lewis acid sites obtained by partial reduction of Ce IV to Ce III cations were responsible for the formation of a CO species at 1725 cm^{-1} which is bonded by its oxygen to the Lewis acid site (Ce III cations) and by its carbon to the noble metal (73). It was also postulated that organometallic complexes with this type of interaction will have corresponding bands in the 1650–1750 cm^{-1} region (92). In addition, the interaction of metal carbonyls with Lewis acid sites leads to a band around 1700 cm^{-1} (93–95). On Pt/SiO_2 promoted with alkalis, CO bound by its carbon to the metal and by its oxygen to the promoter was identified; the corresponding frequencies depended on the nature of the alkali as well as on the reduction temperature of the catalyst (96, 97). We therefore assign the bands at 1750 and 1730 cm^{-1} (Fig. 12C) on the mixed metal catalyst as well as those on Pd/CeO_2 (at 1750 and 1730 cm^{-1}) (Fig. 12A) and those on Co/CeO_2 (at 1750 and 1739 cm^{-1}) (Fig. 12B) catalysts to this type of adsorbed CO. Weak bands at 1920 and 1873 cm^{-1} were attributed to bridging CO.

DISCUSSION

The results obtained by CO and oxygen chemisorption, XPS, XRD, acetaldehyde TPD, and IR for CeO_2, Pd/CeO_2, Co/CeO_2, and $Pd–Co/CeO_2$ catalysts may be outlined as follows.

1. Hydrogen-reduced catalysts contained $Ce^{(3+)}$ in addition to $Ce^{(4+)}$ cations. The presence of $Ce^{(3+)}$ was evidenced by the peaks at Ce($3d$) XPS signals at 885.0 and 903.7 eV, attributed to V′ and U′ peaks, respectively.
2. $Co^{(2+)}$ cations were observed on reduced Co-containing catalysts as evidenced by their Co $2p_{3/2}$ peak at 781.0 eV (and the satellite at about 788 eV) and Co $2p_{1/2}$ at 797 eV (and its satellite at about 804.5 eV).
3. The number of CO molecules adsorbed on the surface of Pd/CeO_2 was almost the same as that of Pd atoms calculated from the XPS signals, indicating that the ratio of CO/Pd was 1 (0.97 experimental value). The ratio CO/Co was also very close to unity (experimental value 0.93). However, the ratio CO/[Pd + Co] for $Pd–Co/CeO_2$ catalyst was equal to ca. 4 (experimental value 3.9), indicating a synergistic effect between Pd and Co when added together on the surface of CeO_2, affecting CO adsorption.
4. Acetyl species (IR band at 1685 cm^{-1}) and η^2 acetaldehyde (Tables 9 and 10) were observed on metal-doped catalysts (Pd/CeO_2, Co/CeO_2, and $Pd–Co/CeO_2$).
5. Acetone desorbed at 630 K on CeO_2 (high temperature desorption) and at 520–560 K (low temperature desorption) on Pd/CeO_2 and $Pd–Co/CeO_2$. On Co/CeO_2, both low temperature and high temperature desorption peaks were observed.

TABLE 9

Vibrational Frequencies (cm^{-1}) for η^2-Acetaldehyde

Mode	Pd/CeO_2[a]	$Pd–Co/CeO_2$[a]	Ru(001)[b,c] (83, 84)	Pd(111)[b] (87)
ν (CO)	1220	1268	1275	1390
ν (CC)	1175	1156	1135–1105	1090
ρ (CH_3)	950	940	975	930

[a] This work.
[b] HREELS.
[c] From ketene.

Acetaldehyde Reactions

Acetaldehyde reactions on the surfaces of CeO_2 and metal (Pd, Co, and Pd–Co)/CeO_2 catalysts are presented in Scheme I. The reduction of acetaldehyde to ethanol (via ethoxides; route 1) on the different catalysts may occur on both metal and oxide sites; this reaction was observed on reduced CeO_2 alone but, as shown by Fig. 15, the ethanol selectivity was highest on Pd/CeO_2.

All catalysts investigated by IR indicated the presence of acetates (route 2 in Scheme I). Oxidation of acetaldehyde to acetates was previously observed on several oxide supports and catalysts such as on ZnO (19), Cu/Zn/Al (25), and TiO_2 (12). On CeO_2 formates were previously observed from methanol (20), and acetates from 2-propanol (98). The oxidation reaction can be described as follows:

$$CH_3CHO\ (a) + O(s) \rightarrow CH_3CHCOO\ (a)$$

$$CH_2CHCOO\ (a) \rightarrow CH_3COO\ (a) + [H]\ (a).$$

Adsorbed acetates will react differently on differently modified CeO_2. Acetates can either decompose to CO_2 and CH_4 (99) or react in a bimolecular ketonization to give acetone and CO_2 (23–25) (route 2a). The first path has been observed on both metals and oxides, the second on oxides only.

During TPD, CH_4 and CO_2 desorbed at 750 K from CeO_2, and from Co/CeO_2 at 750 K and 780 K, respectively, suggesting that these peaks originate from one common surface species (acetates). On $Pd–Co/CeO_2$, CH_4 desorbed first at 450 K then at 615 K together with

TABLE 10

Vibrational Frequencies (ν (CO) Mode) for Adsorbed Acetyl Species

Catalyst	ν(CO) frequency (cm^{-1})
3 wt% Pd/CeO_2 (this work)	1684
3 wt% Co/CeO_2 (this work)	1684
3 wt% Pd, 3 wt% Co/CeO_2 (this work)	1685
Na-Pt/SiO_2 (85)	1684
Pt[a] (83)	1650
$Pd(CH_3CO)$ (89)	1667
Pd[a] (from acetaldehyde) (87)	1565
Pd[a] (from ethanol) (88)	1585
Ni[b] (from methyl acetate) (104)	1517–1528

[a] HREELS.
[b] RAIRS.

CO_2. The first methane desorption peak together with CO desorption is likely from acetaldehyde decomposition on Pd, while the second peak together with CO and CO_2 desorption can be attributed to acetate decomposition. The TPD results indicated that addition of Co did not cause dramatic changes for acetate decomposition on CeO_2. On the other hand, while Pd lowered the decomposition temperature by ca. 100 K, Pd–Co lowered it further by ca. 130 K. Acetone desorption was observed at 630 K on CeO_2 and at 660 K (coincident with propane, route 2b) on Co/CeO_2. This peak is attributed to acetate coupling reactions as presented in route 2a.

IR spectra indicated that surface acetyl species were present (IR bands at 1685 cm^{-1}) only on M/CeO_2 (M: Pd, Co, and Pd–Co), route 3. Acetyl species were previously observed from acetaldehyde on Pd (111) (87), Pt (86), and on Na–Pt/SiO_2 (85). The reaction of acetyl with an adsorbed methyl will give acetone (route 3a); on Pd/CeO_2 part of the acetone is hydrogenated to propane (route 3b). As indicated in Fig. 16, two channels for acetone desorption on these catalysts were observed. On CeO_2,

TABLE 11

ν (CO) Frequencies for CO adsorbed by Its Carbon to the Metal and by Its Oxygen to the Support (MCOS Species: Metal–Carbon–Oxygen Support), on 3 wt% Pd/CeO_2, 3 wt% Co/CeO_2, and 3 wt% Pd, 3 wt% Co/CeO_2 Surfaces

Catalyst	Frequency (cm^{-1})
$Rh/CeO_2/SiO_2$ (73)	1725
Pt–Na/CeO_2 (85)	1776
3 wt% Pd/CeO_2 (this work)	1730, 1750
3 wt% Co/CeO_2 (this work)	1739, 1750
3 wt% Pd, 3 wt% Co/CeO_2 (this work)	1730, 1750
Pd–Na/SiO_2 (96)	1770

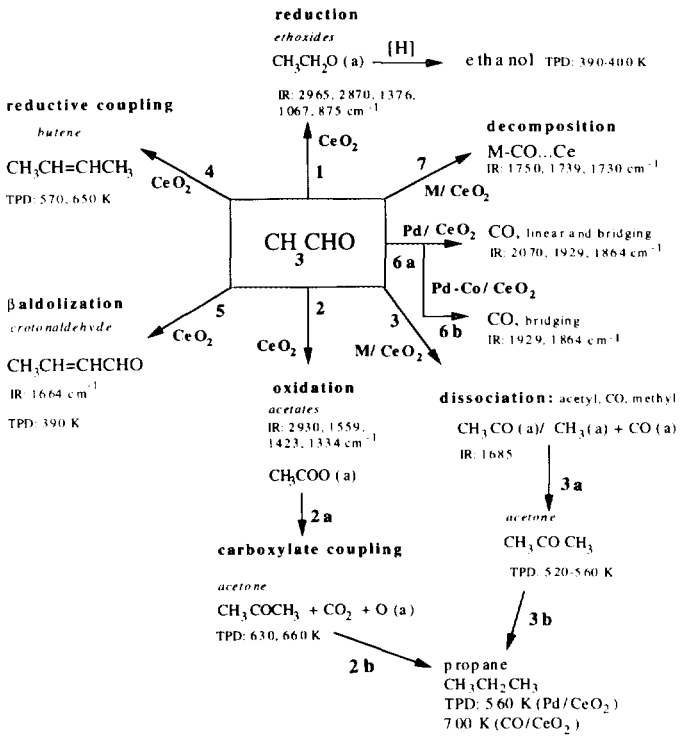

SCHEME I. Acetaldehyde reactions on CeO_2 and M/CeO_2 M: Pd, Co, and Pd–Co.

acetone was formed only from carboxylates (high temperature desorption), on Pd/CeO_2 and Pd–Co/CeO_2 (metal-doped oxide surfaces) acetone was formed only from acetyl reactions (low temperature channel), while on Co/

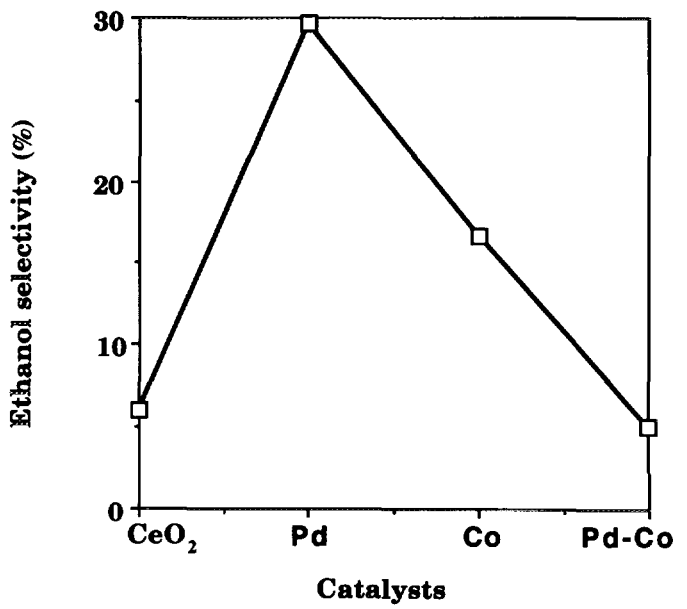

FIG. 15. Ethanol selectivity during acetaldehyde TPD on CeO_2, 3 wt% Co/CeO_2, 3 wt% Pd/CeO_2, and 3 wt% Pd, 3 wt% Co/CeO_2 catalysts.

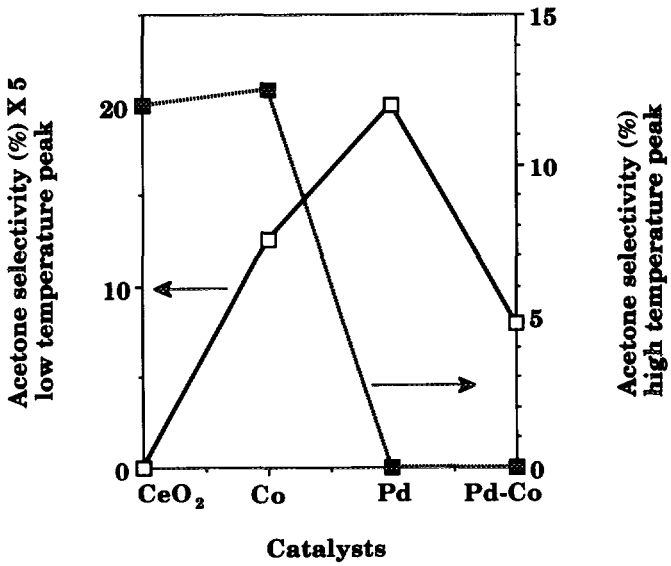

FIG. 16. Acetone selectivity during acetaldehyde TPD on CeO_2, 3 wt% Co/CeO_2, 3 wt% Pd/CeO_2, and 3 wt% Pd, 3 wt% Co/CeO_2 catalysts. The low temperature peak is that at 520–560 K, and the high temperature peak is that at 630 K.

CeO_2 (a partially reduced metal/oxide surface) both desorption channels were observed.

Formation of C_4 Products

Butene and butadiene were observed during acetaldehyde TPD on CeO_2 (combined selectivity = 12%) and to some extent on Co/CeO_2 (4%), route 4. This reaction likely involves the reductive coupling of two molecules of acetaldehyde on adjacent reduced sites on the surface:

$$2CH_3CHO\,(a) + n\,Ce^{x+} \rightarrow CH_3CH{=}CHCH_3 + n\,Ce^{x+4/n} + 2O(a).$$

Butadiene is most likely formed by further dehydrogenation of butene. Reductive coupling of carbonyls (aldehydes and ketones) is known in inorganic chemistry and occurs in slurries of reduced metals (such as $TiCl_4$, $TiCl_3$, and VCl_3 plus reducing agents) (14, 15). This reaction is analogous to carbonyl coupling to pinacolates which occurs on several reduced metals (such as $TiCl_4$, VCl_3, Ce/I_2); for Ce/I_2 systems the active sites is believed to be Ce^{2+} cations (14). This stoichiometric liquid–solid reaction was also observed as a gas–solid reaction during TPD of several aldehydes (acetaldehyde (16, 100), acrolein (16), benzaldehyde (16, 17)) and ketones (cyclohexanone, cyclohexenone, and *p*-benzoquinone (101)) on the surfaces of reduced (sputtered) TiO_2 (001) single crystals.

Cross-coupling between two aldehydes was also observed on "hydrogen-reduced" CeO_2 (18). However, it should be noted that some reactions in heterogeneous catalytic systems might occur through that mechanism; one can think of the Lebedev process (102) where butadiene is selectively formed from ethanol in one step on $MgO–SiO_2$ catalysts (ethanol dehydrogenation to acetaldehyde on SiO_2 at 670 K is very selective, 92+%, (103)). The selectivity to C_4 hydrocarbons on all catalysts in this study is presented in Fig. 17.

Crotonaldehyde and crotyl alcohol were the result of β-aldolization of CH_3CHO on the surface of CeO_2 (route 5). Aldolization of acetaldehyde was previously observed on other surfaces including Cu/Zn/Al catalysts (25), TiO_2 powders (12), and single crystals (18). It requires, in addition to Lewis acid sites at which to bind two molecules of acetaldehyde, a base site to abstract a hydrogen atom from the α position of the carbonyl. TPD of acetaldehyde on CeO_2 produced a 48% selectivity to crotonaldehyde and crotyl alcohol, this is compared to 93.7% on TiO_2 powder (12) and 50.5% on Cu/Zn/Al (25). Addition of Co or Pd decreased acetaldehyde aldolization (Fig. 17) partly because acetaldehyde tends to react directly on the metal to give ethanol (among other products) and partly because metal addition resulted in further reduction of the surface of CeO_2 which, as indicated by IR (Figs. 12 and 15), inhibited the formation of crotonaldehyde when the catalyst was reduced at 674 K.

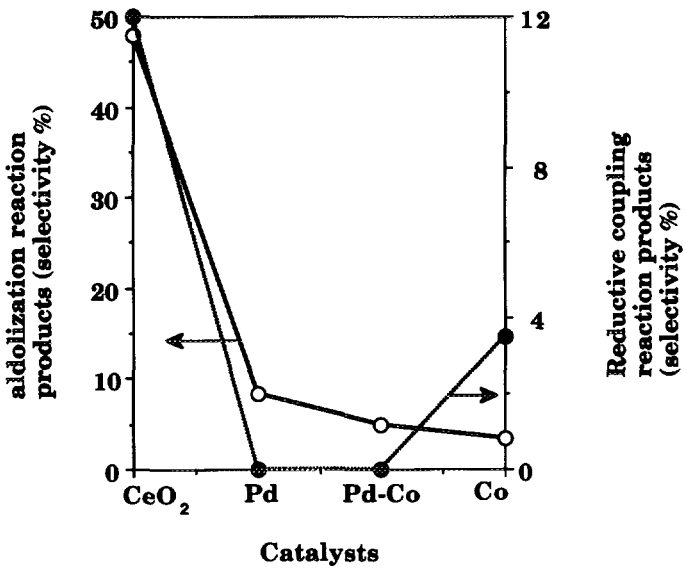

FIG. 17. Products of aldolization reaction (crotonaldehyde and crotyl alcohol) and of reductive coupling (butene, and butadiene) during acetaldehyde TPD on CeO_2, 3 wt% Co/CeO_2, 3 wt% Pd/CeO_2, and 3 wt% Pd, 3 wt% Co/CeO_2 catalysts.

CO Formation

The formation of CO from acetaldehyde decomposition was previously observed on Pd (111) (87), Rh (111) (81), and Pt (111) (86). In this study linear (L) and bridging (B) bands of CO were observed on Pd/CeO_2 (L, 2070 cm^{-1}; B, 1929, 1864 cm^{-1}), route 6a, while only B bands were observed on $Pd–Co/CeO_2$ (1920, 1873 cm^{-1}), route 6b; no B or L bands were observed on Co/CeO_2. In addition, bands at 1750, 1739 cm^{-1} (Co/CeO_2) and at 1750, 1730 cm^{-1} (on Pd/CeO_2 and $Pd–Co/CeO_2$) were observed (route 7). These bands are attributed to CO adsorbed by its carbon to the metal and by its oxygen to an oxygen-deficient site of the oxide such as Ce^{3+}; this configuration might be called MCOS (M for metal, C for carbon, O for oxygen, and S for support); M-CO . . . Ce^{x+}, $x < 4$). These bands were previously observed on several surfaces of noble metal catalysts with and without alkalis and rare earth oxide promoters; their assignments were based, as indicated above, on organometallic complexes of metal carbonyls with Lewis acid sites (92–95). A comparison between the bands observed in this study and those reported in the literature is presented in Table 11.

CONCLUSIONS

The surface and bulk composition of CeO_2, Co/CeO_2, Pd/CeO_2, and $Pd–Co/CeO_2$ were investigated by XRD, XPS, and chemisorption. Reduction of CeO_2 by hydrogen was indicated in XPS by the presence of Ce(3*d*) signals at 885.0 and 903.7 eV attributed to V′ and U′ peaks of $Ce^{(+3)}$ cations. The amount of oxygen adsorbed on CeO_2 (reduced at 673 K) was 5×10^{14} atoms/cm^2. $Co^{(2+)}$ cations were present on both Co/CeO_2 and $Pd–Co/CeO_2$ catalysts, as evidenced by the Co $2p_{3/2}$ and $2p_{1/2}$ lines at 781.0 and 797.0 eV and their corresponding satellites at about 788.0 and 804.0 eV, respectively. The reactions of acetaldehyde on the surfaces of these catalysts were studied by TPD and FT-IR and are summarized in Scheme I. Acetaldehyde reduction to ethanol, via ethoxides, was observed on all catalysts; the highest extent of reduction to ethanol was observed on Pd/CeO_2. Four types of C–C bond formation were observed: (i) β-aldolization to crotonaldehyde and crotyl alcohol; (ii) carboxylate ketonization to acetone; (iii) acetyl reaction with adsorbed methyl to give, also, acetone (this reaction was observed only on Pd/CeO_2, Co/CeO_2, and $Pd–Co/CeO_2$ catalysts); and (iv) reductive coupling of two molecules of acetaldehyde to form butenes and butadiene. Several adsorbed species were observed. In addition to ethoxides and carboxylate species observed on all catalysts, on metal-doped surfaces acetyl species (1684 cm^{-1}), adsorbed acetaldehyde η^2 (C, O), and CO adsorbed by its carbon to Pd, Co, or Pd–Co and by oxygen to reduced Ce cations (MCOS) were observed. In general, $Pd–Co/CeO_2$ was similar to Pd/CeO_2 for acetaldehyde reactions but more active (86% of adsorbed acetaldehyde, at saturation, was converted). The conversion of acetaldehyde by this catalyst exceeded that of Pd/CeO_2 and Co/CeO_2. The high activity of the $Pd–Co/CeO_2$ catalyst suggests its potential for aldehyde destruction.

REFERENCES

1. Sakugawa, H., and Kaplan, I. R., *Atmos. Environ.* **27B**, 203 (1993).
2. Roberts, J. M., *Atmos. Environ.* **24A**, 243 (1990).
3. Graedel, T. E., Mandich, M. L., and Weschler, C. J., *J. Geophys. Res.* **91**, 5205 (1986).
4. Rajesh, H., and Ozkan, U. S., *Ind. Eng. Chem. Res.* **32**, 1622 (1993).
5. McCabe, R. W., and McReady, D. F., *Chem. Phys. Lett.* **111**, 89 (1984).
6. McCabe, R. W., and Mitchell, P. J., *Appl. Catal.* **44**, 73 (1988).
7. Lapinski, M. P., Silver, R. G., Ekerdt, J. G., and McCabe, R. W., *J. Catal.* **105**, 258 (1987).
8. Foster, J. J., and Masel, R. I., *Ind. Eng. Chem. Proc. Res. Dev.* **25**, 2556 (1986).
9. Altshuller, A. P., *Atmos. Environ.* **27A**, 21 (1993).
10. Graedel, T. E., Hawkins, D. T., and Claxton, L. D., "Atmospheric Chemical Compounds Sources, Occurrence, and Bioassay," Academic Press, San Diego (1987).
11. Nunan, J. G., Bogdan, C. E., Klier, K., Smith, K. J., Yong, C. W., and Herman, R. G., *J. Catal.* **113**, 410 (1988).
12. Idriss, H., Kim, K. S., and Barteau, M. A., *J. Catal.* **139**, 119 (1993).
13. U.S. Patent 3,948,991 (1982).
14. Kahn, B. E., and Rieke, R. D., *Chem. Rev.* **88**, 733 (1988).
15. McMurry, J. E., *Chem. Rev.* **89**, 1513 (1989).
16. Idriss, H., Pierce, K., and Barteau, M. A., *J. Am. Chem. Soc.* **113**, 715 (1991).
17. Idriss, H., Pierce, K., and Barteau, M. A., *J. Am. Chem. Soc.* **116**, 3063 (1994).
18. Idriss, H., Libby, M., and Barteau, M. A., *Catal. Lett.* **15**, 13 (1992).
19. Vohs, J. M., and Barteau, M. A., *Langmuir* **5**, 965 (1989).
20. Lamotte, J., Morávek, V., Bensitel, M., and Lavalley, J. C., *React. Kinet. Catal. Lett.* **36**, 113 (1988).
21. Idriss, H., Kim, K. S., and Barteau, M. A., *Surf. Sci.* **262**, 113 (1992).
22. Idriss, H., Hindermann, J. P., Kieffer, R., Kiennemann, A., Vallet, A., Chauvin, C., Lavalley, J. C., and Chaumette, P., *J. Mol. Catal.* **90**, 183 (1987).
23. Kim, K. S., and Barteau, M. A., *J. Catal.* **125**, 353 (1990).
24. Idriss, H., Kim, K. S., and Barteau, M. A., *Stud. Surf. Sci. Catal.* **64**, 327 (1991).
25. Kiennemann, A., Idriss, H., Kieffer, R., Chaumette, P., and Durand, D., *Ind. Eng. Chem. Res.* **30**, 1130 (1991).
26. Claridge, J. B., Green, M. L. H., Tsang, S. C., and York, A. P. E., *J. Chem. Soc. Farad. Trans.* **89**, 1089 (1993).
27. Orita, H., Naito, S., and Tamaru, K., *J. Catal.* **90**, 183 (1984).
28. Ichikawa, M., *CHEMTECH* **12**, 674 (1982).
29. Ichikawa, M., Fukushima, T., Shikakura, K., and Kanegawa, J., "Proceeding, 8th International Congress on Catalysis, Berlin, 1984." Dechema, Frankfort-am-Main, 1984.
30. Lippert, S., Baumann, W., and Thomke, K., *J. Mol. Catal.* **69**, 199 (1991).

31. Beck, D. D., Capehart, T. W., and Hoffman, R. W., *Chem. Phys. Lett.* **159,** 207 (1989).
32. Arai, T., Maruya, K.-I., Domen, K., and Onishi, T., *J. Catal.* **141,** 533 (1993).
33. Gonzalez-Elipe, A. R., Fernandez, A., Holgado, J. P., Caballero, A., and Munuera, G., *J. Vac. Sci. Technol. A* **11,** 58 (1993).
34. Diagne, C., Idriss, H., Pepin, I., Hindermann, J. P., and Kiennemann, A., *Appl. Catal.* **50,** 43 (1989).
35. Diagne, C., Idriss, H., Hindermann, J. P., and Kiennemann, A., *Appl. Catal.* **51,** 165 (1989).
36. Nunan, J. G., Robota, H., Cohn, M., and Bradley, S. A., *J. Catal.* **133,** 309 (1992).
37. Lööf, P., Kasemo, B., and Keck, K.-E., *J. Catal.* **118,** 339 (1989).
38. Miki, T., Ogawa, T., Haneda, M., Kakuta, N., Ueno, A., Tateishi, S., Matsura, S., and Sato, M., *J. Phys. Chem.* **94,** 6464 (1990).
39. Belousov, V. M., Stoch, J., Batcherikova, I. V., Rozhkova, E. V., and Lyashenko, L. V., *Appl. Surf. Sci.* **35,** 481 (1988–1989).
40. Idriss, H., Diagne, C., Hindermann, J. P., Kiennemann, A., and Barteau, M. A., "Proceedings 10th International Congress on Catalysis, Budapest, 1992" (L. Guczi, F. Solymosi, and P. Tetenyi, Eds.). Akadémiai Kiadó, Budapest, 1993.
41. Bernal, S., Calvino, J. J., Ciferdo, G. A., Rodriguez-Izquierdo, J. M., and Perrichon, V., Laachir, A., *J. Catal.* **137,** 1 (1992).
42. Le Normand, J. F., Hilaire, L., Kili, K., Krill, G., and Maire, G., *J. Phys. Chem.* **92,** 2561 (1988).
43. Klug, H. P., and Alexander, L. E. "X-ray Diffraction Procedures for Polycrystalline and Amorphous Materials." Wiley New York, 1954.
44. Czerwinski, F., and Smeltzer, W. W., *J. Electrochem. Soc.* **140,** 2606 (1993).
45. Ko, E. I., Benziger, J. B., and Madix, M. A., *J. Catal.* **62,** 264 (1980).
46. Hollenstein, H., and Gunthard, H., *Spectrochim. Acta* **27A,** 2027 (1971).
47. Wulser, K. W., and Langell, M. A., *Catal. Lett.* **15,** 39 (1992).
48. Rocker, G., and Göpel, W., *Surf. Sci.* **181,** 530 (1987).
49. Hoang, M., Hughes, A., and Turney, T. W., *Appl. Surf. Sci.* **72,** 55 (1993).
50. Graham, G. W., Schmitz, P. J., Usmen, R. K., and McCabe, R. W., *Catal. Lett.* **17,** 175 (1993).
51. Paparazzo, E., *Surf. Sci.* **234,** L253 (1990).
52. Akai, T., Maruya, K.-I., Domen, K., and Onishi, T. *J. Catal.* **141,** 533 (1993).
53. Padeste, C., Cant, N. W., and Trimm, D. L., *Catal. Lett.* **18,** 305 (1993).
54. Greaser, D. A., Harison, P. G., Morris, M. A., and Wolgindale, B. A., *Catal. Lett.* **23,** 13 (1994).
55. Dauscher, A., Weher, P., and Hilaire, L., *Catal. Lett.* **14,** 171 (1992).
56. Le Normand, F., El-Fallah, J., Hilaire, L., Légaré, P., Kotani, A., and Parlebas, J. C., *Solid State Commun.* **71,** 885 (1989).
57. Braatem, N. A., Grestad, J. K., and Raaen, S., *Surf. Sci.* **222,** 499 (1989).
58. Strydom, C. A., and Strydom, H. J., *Inorg. Chimica Acta* **161,** 7 (1989).
59. Bak, K., and Hilaire, L., *Appl. Surf. Sci.* **70/71,** 191 (1993).
60. Praline, G., Koel, B. E., Hance, R. L., Lee, H.-I., and White, J. M., *J. Elect. Spect. Rel. Phenom.* **21,** 17 (1980).
61. Belton, D. N., and Schmieg, S. J., *J. Vac. Sci. Technol. A* **11,** 2330 (1993).
62. Zsoldos, Z., Sàrkàny, A., and Guczi, L., *J. Catal.* **145,** 235 (1994).
63. Otto, K., Haack, L. P., and de Vires, J. E., *Appl. Catal. B* **1,** 1 (1992).
64. Shelef, M., Haack, L. P., Soltis, R. E., deVires, J. E., and Logothetis, E. M., *J. Catal.* **137,** 114 (1992).
65. Fallier, M., Thomas, J. P., Frigerio, J. M., and Rivory, J., *Solid State Commun.* **57,** 59 (1986).
66. Fries, S. M., Wagner, H.-G., Campbell, S. J., Gonser, U., Bales, J., and Steiner, P., *J. Phys. F* **15,** 1193 (1985).
67. Aubertine, F., Gonser, U., and Campbell, S. J., *J. Phys. F* **15,** 2069 (1985).
68. Chuang, T. J., Brundle, C. R., and Rice, D. W., *Surf. Sci.* **59,** 413 (1976).
69. Fierro, G., Dragone, R., Moretti, G., and Porta, P., *Surf. Int. Anal.* **19,** 565 (1992).
70. Oku, M., and Sato, Y., *Appl. Surf. Sci.* **55,** 37 (1992).
71. Scofield, J. H., *J. Electr. Spec. Rel. Phenom.* **8,** 129 (1976).
72. Kerkhof, F. P. J. M., and Moulijn, J. A., *J. Phys. Chem.* **83,** 1612 (1979).
73. Minachev, K. H. M. and Shpiro, E. S., *in* "Catalyst Surface: Physical Methods of Study" (K. H. M. Minachev and E. S. Shpiro, Eds.), p. 244. CRC Press, Moscow; Boca Raton, FL, 1990.
74. Davis, J. L., and Barteau, M. A., *Langmuir* **5,** 1229 (1989).
75. Lavalley, J. C., Saussey, J., Lamotte, J., Breault, R., Hindermann, J. P., and Kiennemann, A., *J. Phys. Chem.* **94,** 5941 (1990).
76. Trautman, S., Barens, M., and Auroux, A., *J. Catal.* **136,** 613 (1992).
77. Jackson, P., and Parfitt, G. D., *J. Chem. Soc., Farad. Trans.* **68,** 1443 (1972).
78. Munuera, G., and Carrizosa, I., *Acta. Cient. Venez. Suppl.* **2,** 226 (1973).
79. Bowker, M., Houghton, H., and Waugh, K. C., *J. Catal.* **79,** 431 (1987).
80. Bréault, R. Ph.D. dissertation, Université de Strasbourg, 1986.
81. "Handbook of Data of Organic Compounds," 2nd ed., Vol 3, HODOC 8930, p. 1556 (1986).
82. Waghary, A., and Blackmond, D. G., *J. Phys. Chem.* **97,** 6002 (1993).
83. Mc Clellan, M. R., Gland, J. L., and Mc Feeley, F. R., *Surf. Sci.* **112,** 63 (1981).
84. Houtman, C. J., and Barteau, M. A., *J. Catal.* **130,** 528 (1991).
85. Jin, T., Zhou, Y., Mains, G. J., and White, J. M., *J. Phys. Chem.* **91,** 5931 (1987).
86. Henderson, M. A., Radloff, P. L., White, J. M., and Mims, C. A., *J. Phys. Chem.* **92,** 4111 (1988).
87. Henderson, M. A., Zhou, Y., and White, J. M., *J. Am. Chem. Soc.* **111,** 1185 (1989).
88. Boujana, S., Demri, D., Cressely, J., Kiennemann, A., and Hindermann, A., *Catal. Lett.* **7,** 359 (1990).
89. McCabe, R. W., Di Maggio, C. L., and Madix, R. J., *J. Phys. Chem.* **89,** 854 (1985).
90. Davis, J. L., and Barteau, M. A., *J. Am. Chem. Soc.* **111,** 1782 (1989).
91. Davis, J. L., and Barteau, M. A., *Surf. Sci.* **235,** 235 (1990).
92. Adams, D. M., and Booth, G., *J. Chem. Soc.* 1112 (1962).
93. Heiber, W., Braun, G., and Beck, W., *Chem. Ber.* **93,** 901 (1960).
94. Durfee, L. D., and Rothwell, I. P., *Chem. Rev.* **88,** 1059 (1988) and references therein.
95. Horwitz, C. P., and Shriver, D. F., *Adv. Org. Chem.* **23,** 219 (1984).
96. Ulmer, S. W., Skarstad, P. M., Burlitch, J. M., and Hughes, R. E., *J. Am. Chem. Soc.* **95,** 4469 (1973).
97. Crease, A. E., and Legzdins, P., *J. Chem. Soc. Chem. Comm.* 268 (1972).
98. Kotz, J. C., and Turnipseed, C. D., *J. Chem. Soc. Chem. Comm.* 41 (1970).
99. Pitchon, V., Primet, M., and Praliaud, H., *Appl. Catal.* **62,** 317 (1990).

100. Gravelle-Rumeau-Maillot, M., Pitchon, V., Martin, G. A., and Praliaud, H., *Appl. Catal. A* **98,** 45 (1993).
101. Zaki, M. I., Hussein, G. A. M., El-Ammawy, H. A., Mansour, S. A. A., Polz, J., and Knözinger, H., *J. Mol. Catal.* **57,** 367 (1990).
102. Barteau, M. A., Bowker, M., and Madix, R. J., *J. Catal.* **647,** 118 (1981).
103. Idriss, H., and Barteau, M. A. Extended Abstracts-24, Materials Research Society Meeting, Boston, p. 127 (1990).
104. Idriss, H., and Barteau, M. A., *Stud. Surf. Sci. Catal.* **78,** 463 (1993).
105. Weissermel, K., and Arpe, H.-J. "Industrial Organic Chemistry," p. 94. Verlag Chemie, 1978.
106. Matsumura, Y., Hashimoto, K., and Yokoshida, S., *J. Chem. Soc. Chem. Commun.* 1599 (1987).
107. Zahidi, E., Castonguay, M., and McBreen, P., *J. Am. Chem. Soc.* **116,** 5847 (1994).